DE LA RECHERCHE À L'INDUSTRIE

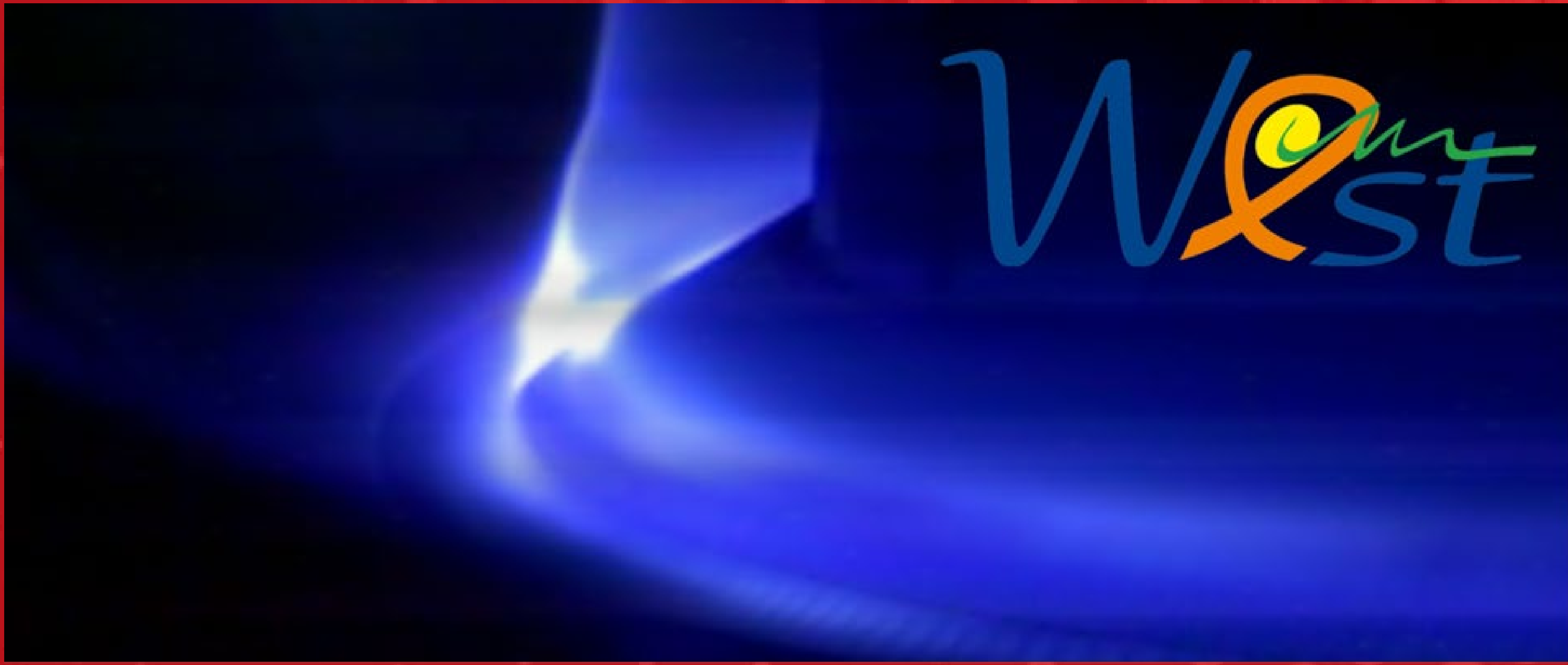

Numerical study and control of divertor detachment: impact of divertor geometry, particle and energy sources

Hao YANG et al.

Outline

- Background
- Numerical modeling
- Detachment characteristics
- Impact of divertor closure/impurity
- Simplified model
- Detachment control
- Conclusion

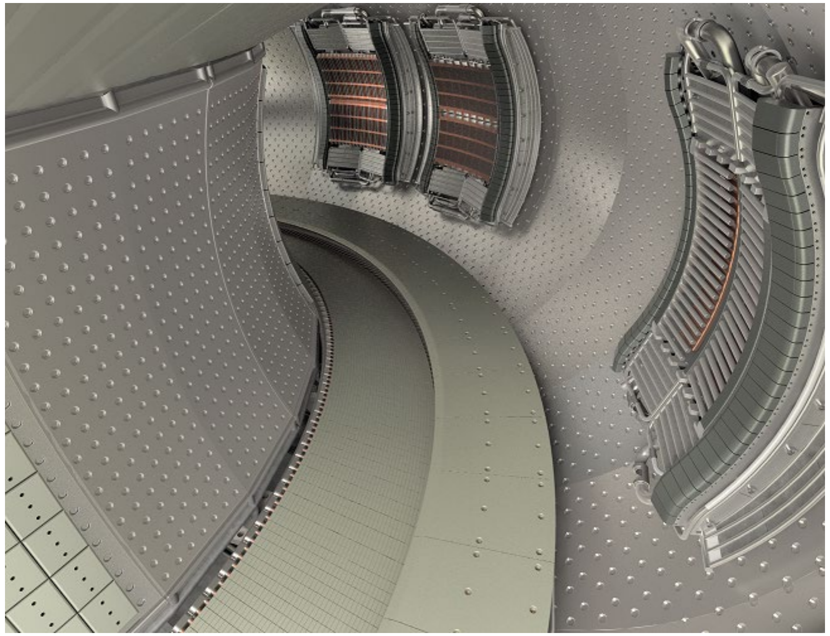

The interior of Tokamak West

Background

Background [*see for ex. C,S,Pitcher & P,C,Stangeby. (1997) 779–930*] :

- Divertor: plasma-wall interaction and the exhaust of heating power (~40 MW/m^2 for ITER)
- Detachment: spreading power over larger surfaces through radiation and keeping target heat loads at manageable levels (≤10 MW/m2)
- Raising plasma density, impurity seeding, input power
- Erosion and melting of edge structure are reduced when detached

Difficulties:

- Deep detachment may lead to a reduction in the performance of core plasma
- Control of degree of detachment
- Measurements

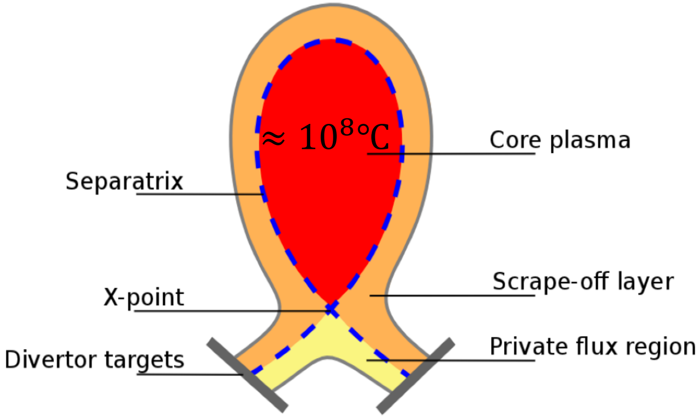

Divertor configuration

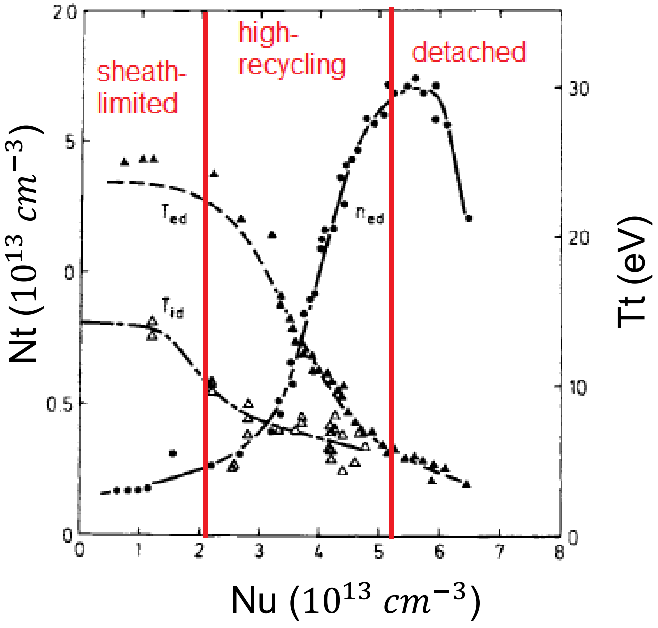

Numerical tools: SOLEDGE-EIRENE

- Predicting edge plasma properties
- Fluid model
- Multi-species Zhdanov closure
- Kinetic neutrals implemented via coupling to EIRENE
- Immersed boundary condition methods, enabling simulations with complex wall geometries

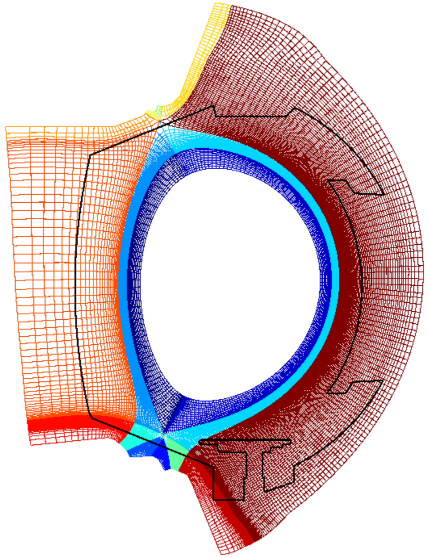

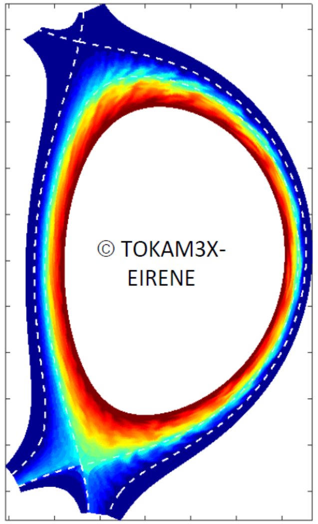

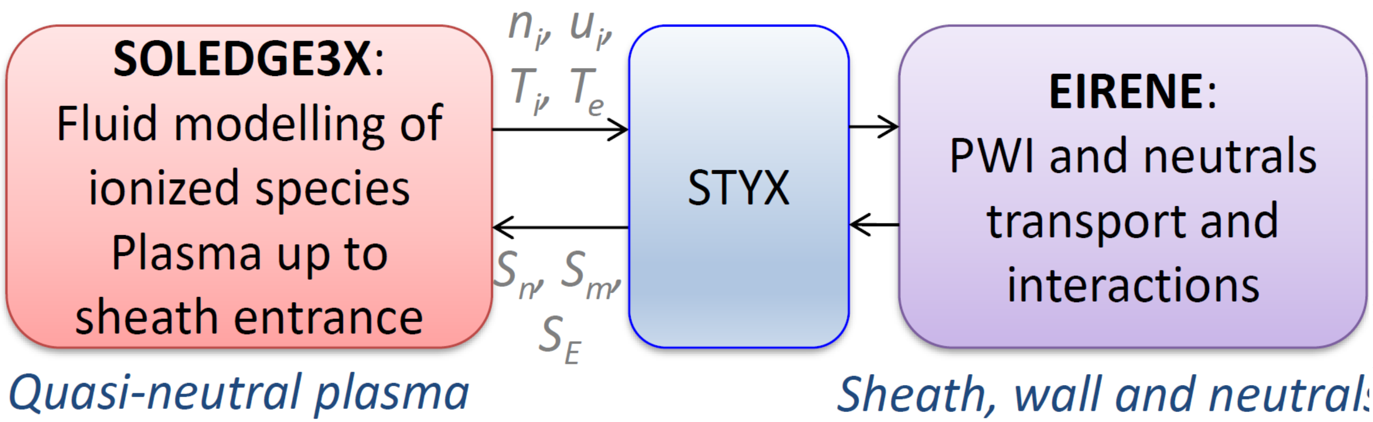

SOLEDGE3X: Fluid modelling of ionized species Plasma up to sheath entrance

n_i, u_i, T_i, T_e →

← S_n, S_m, S_E

STYX

EIRENE: PWI and neutrals transport and interactions

Quasi-neutral plasma

Sheath, wall and neutrals

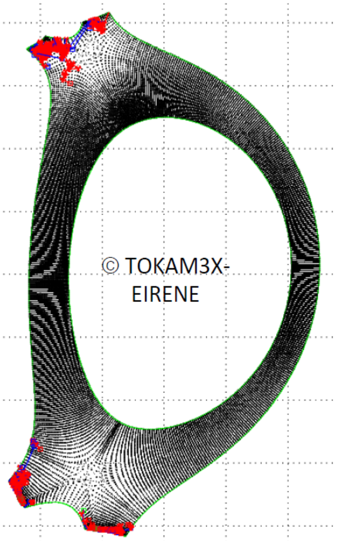

H. Bufferand et al NME 18 (2019), p. 82-86

Numerical tools: Simulation control script

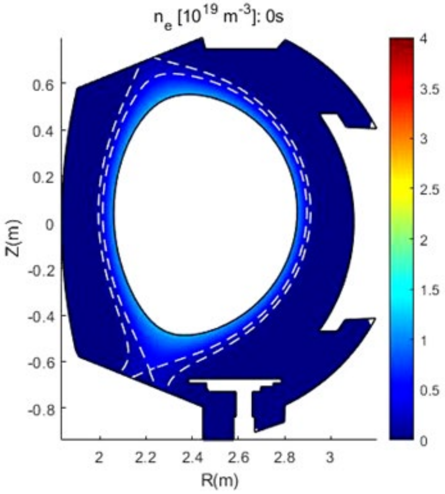

- Be able to mimic the operation in the experiment
- Control multiple parameters with feedback (time delay, radial profile, diff map)
- FD 5-10 times faster than constant puff rate to reach a steady state
- Manage the calculation resources

$$\text{Puff rate} = k_n\left(k_P * e(t) + k_i * \int e(t)\,dt + kd * \frac{d}{dt}e(t)\right) + bg$$

$e(t) = \text{measured value} - \text{target value}$

$k_n = \text{normalized factor}$

$k_P = \text{proportional gain}$

$k_i = \text{integral gain}$

$k_d = \text{derivative gain}$

$bg = \text{background value}$

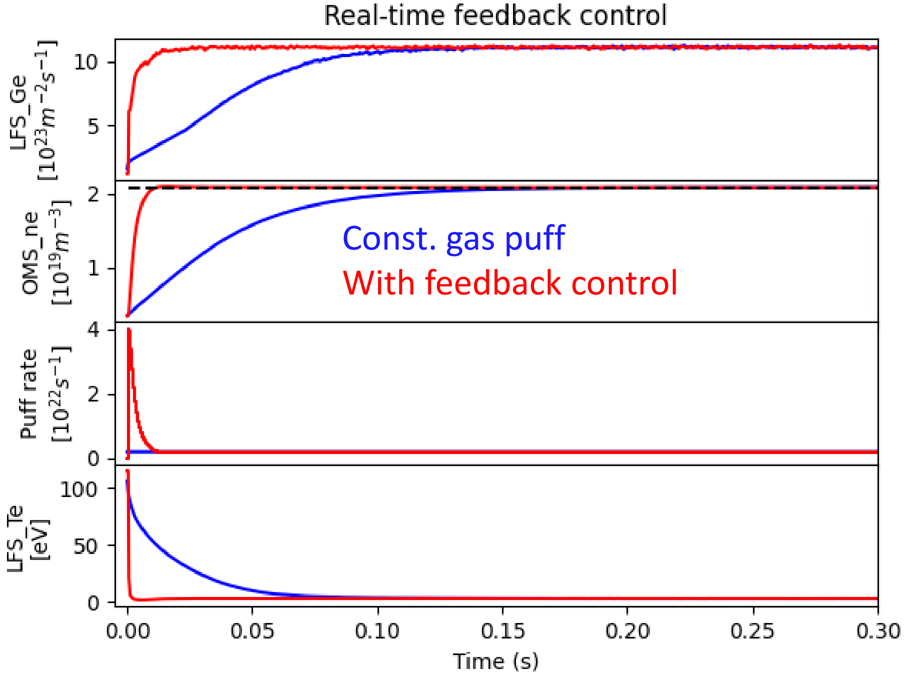

Numerical modeling: WEST L-mode

Operation parameters of WEST #56420@7.3s in C5 campaign

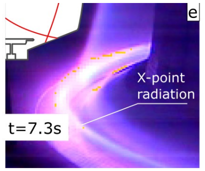

Major radius R_0 (m)	2.5
Minor radius a (m)	0.4
Plasma volume (m^3)	15
Plasma current I_p(MA)	0.6
Toroidal field B_t(T) @ R_0	3.6
Heating power $P_{in,total}$(MW)	0.663
Core radiated power P_{rad}^{core}(MW)	0.168
Upstream separatrix density (1e19/m^3)	2.47

Simulation setups

1) Pure deuterium
2) $n_{e,sep}$ = 2.47 [10^{19}/m^3] (D puff Feed-back control)
3) Input power $P_{in} = P_{heat} - P_{rad}^{core} \simeq 0.45$ [MW]
4) $\chi_e = \chi_i = D_\perp/0.3, \nu = 0.3$ [m^{2}s^{-1}]
5) Recycling coefficient R_{wall} = 1, V_{pump} = 35 [m^{3}s^{-1}]
6) Drifts (ExB, GradB, CurvB), Ballooning

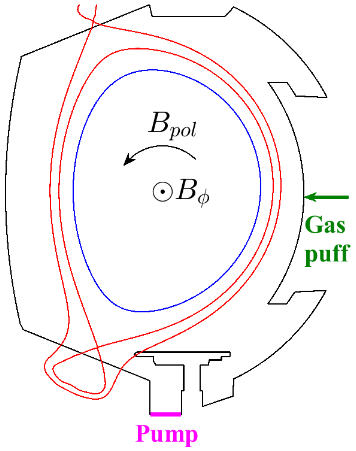

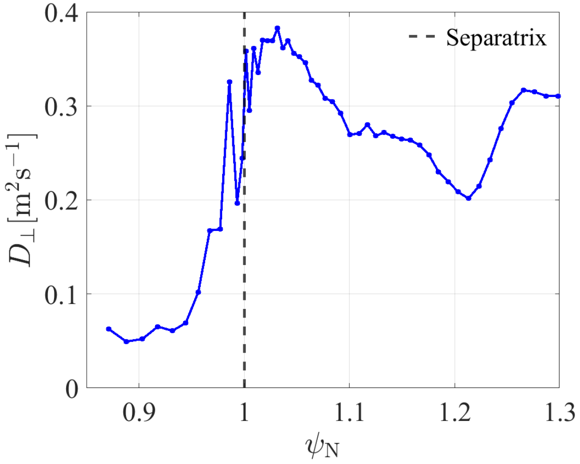

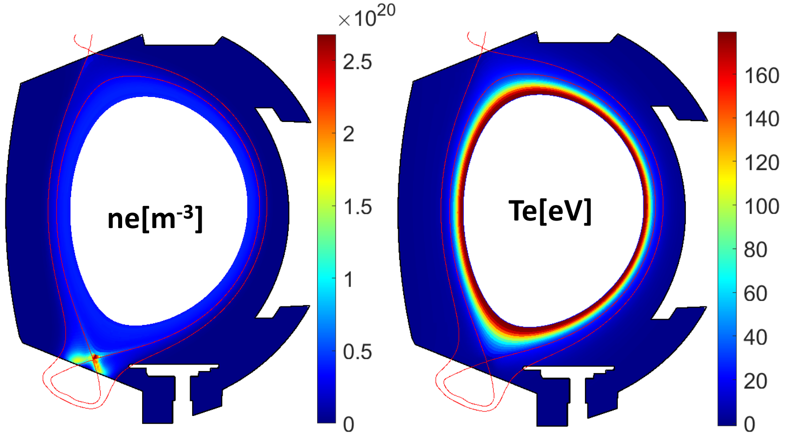

OMP

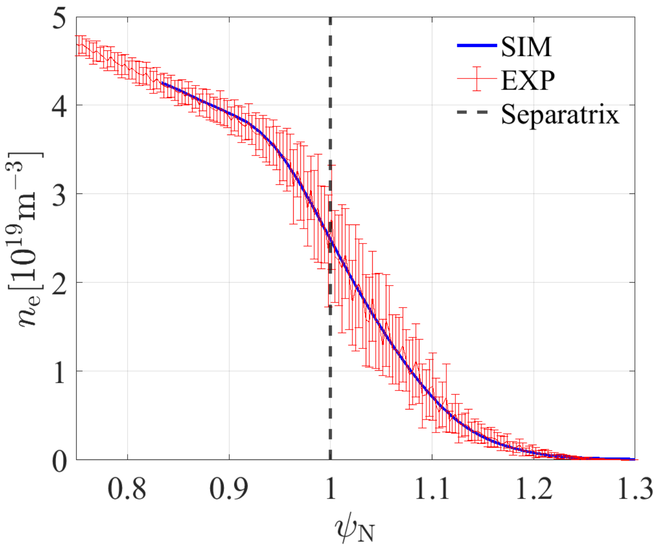

Inner target

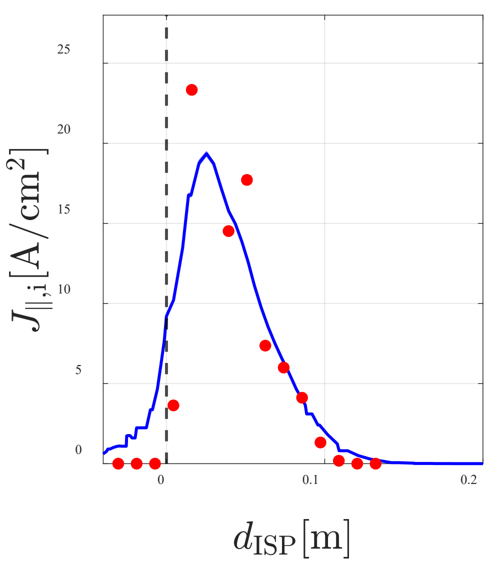

Outer target

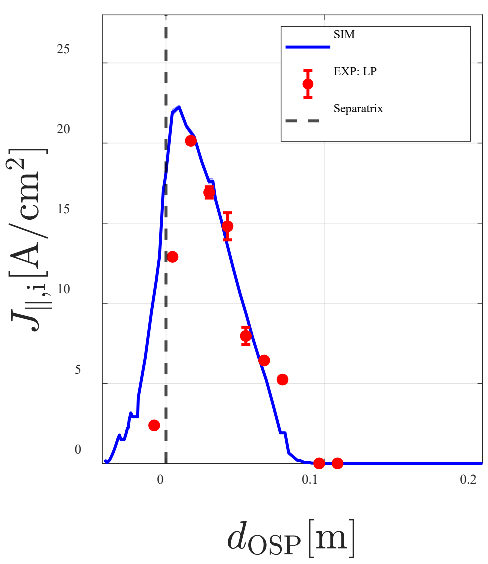

Numerical modeling: WEST L-mode, real-time scan

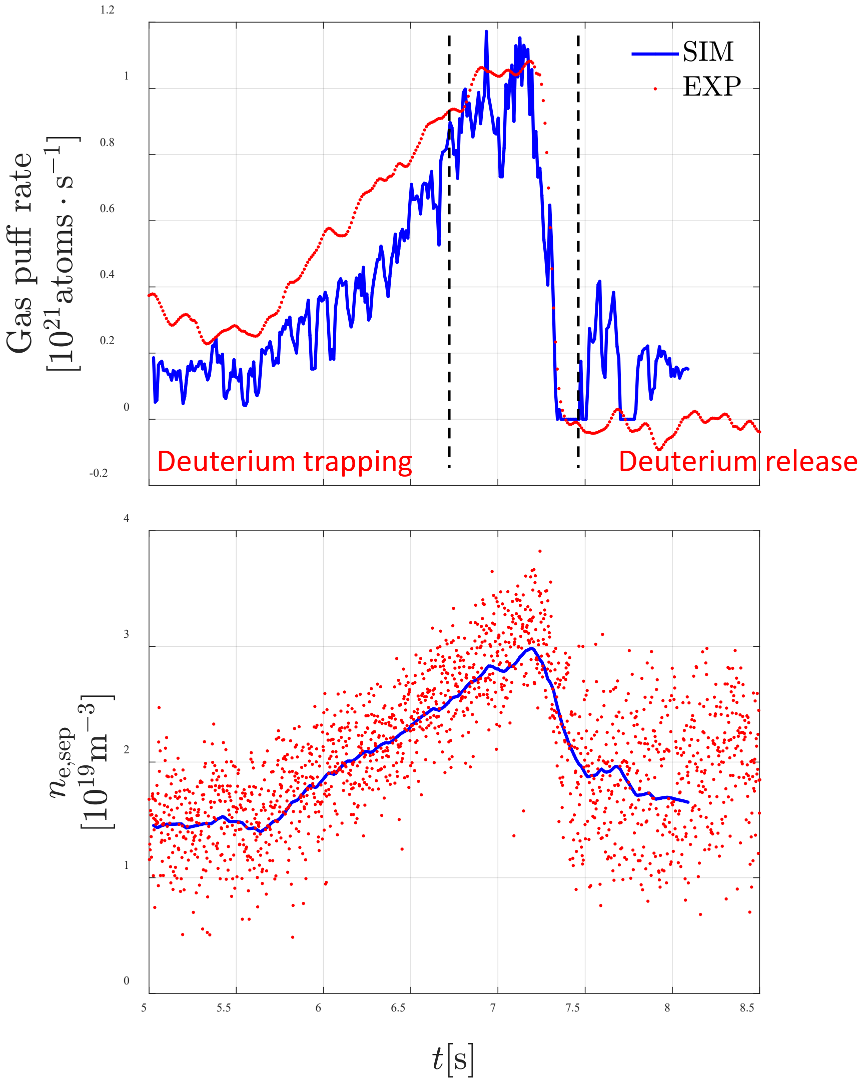

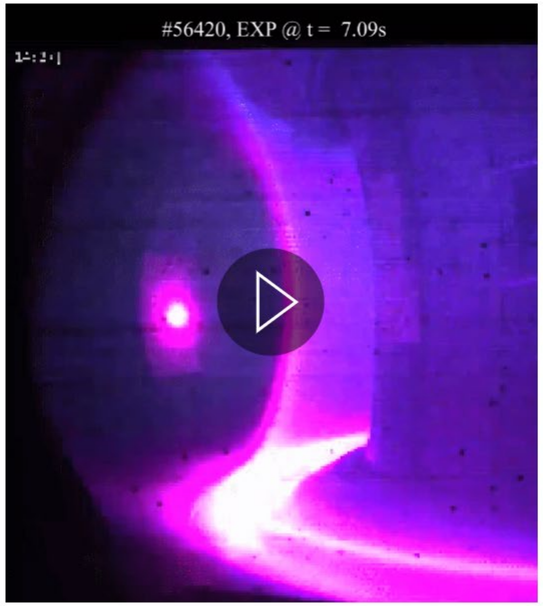

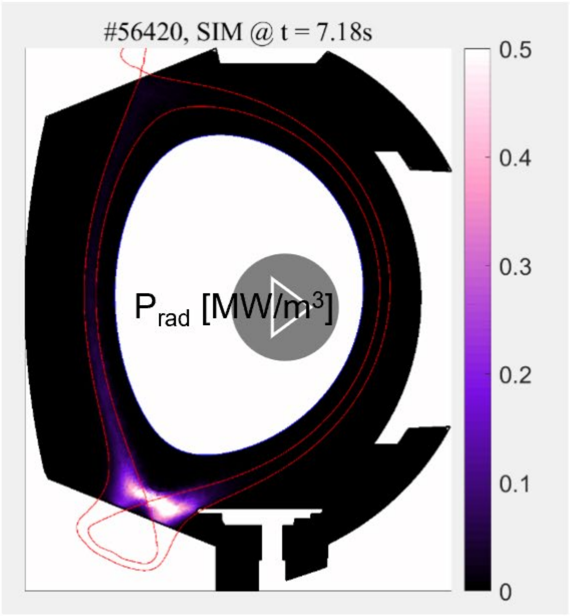

- Wall saturate state can influence the relationship between gas puff and plasma density
- Numerical simulation can reproduce the detachment process close to the one in real experimental shots

Numerical modeling: TCV H-mode

Simulation setups

Reference shot number	#70690@t=1s
Plasma composition	**D,C**
Recycling coefficients	Rwall,D = 0.99 Rwall,C = 0.5
Pedestal temperature	**Ti = Te = 405eV**
Upstream electron density (/m3)	1.36e19
Drifts	No
Transport coefficients	Diff $\propto P_{neu}/B$ $\chi_{\perp,i}, \chi_{\perp,e}$ non-constant $\chi_{\perp,i}$ = $2\chi_{\perp,e}$ inside LCFS $\boldsymbol{\nu}$ = 0.2 m^2/s
Sputtering	The physical: Bohdansky model The chemical: Roth model

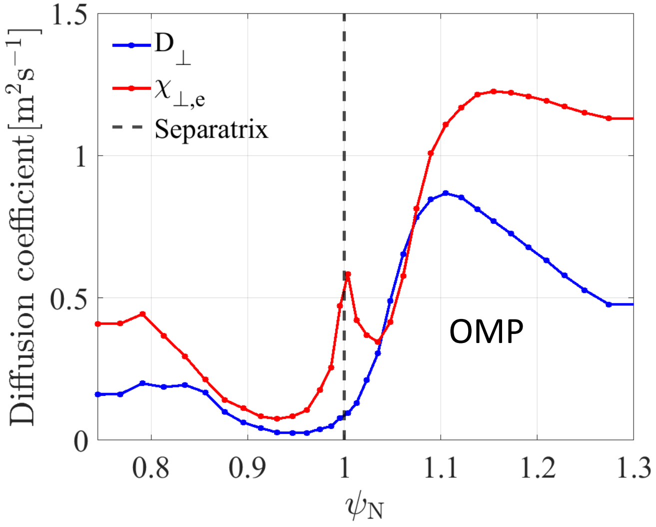

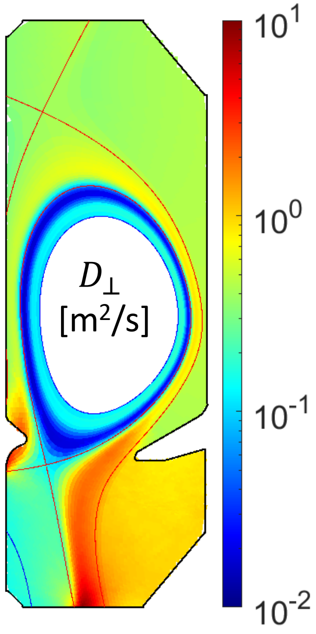

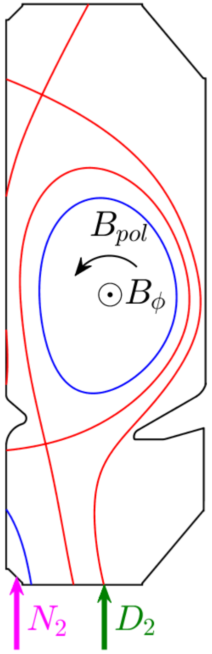

Numerical modeling: TCV H-mode

Results

Para	SIM	EXP
Input power[kW] (npsi >=0.8)	Pin,e = 76KW Pin,i = 137 KW	Pin,total ~251KW
Sputtering estimation	2.87% (outer strike point) 3.90% (inner strike point)	-
$P_{neu,baffle}$ [mPa]	36.8	34-36
$P_{neu,omp}$ [mPa]	0.7	1-10

P_{neu} recalculated based on M Wensing et al 2019 PPCF 61 085029

Electron density [1e19/m³]

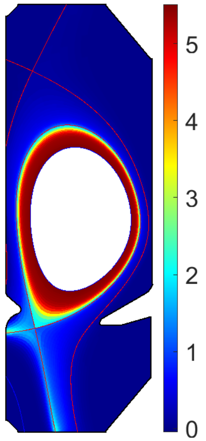

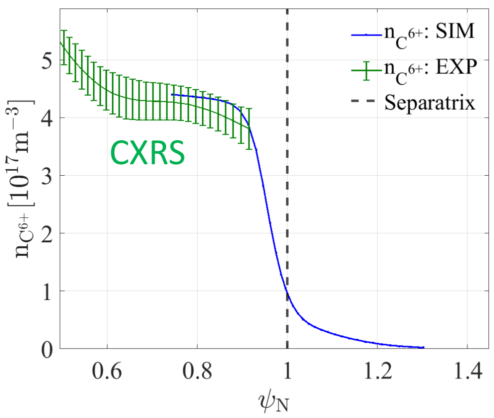

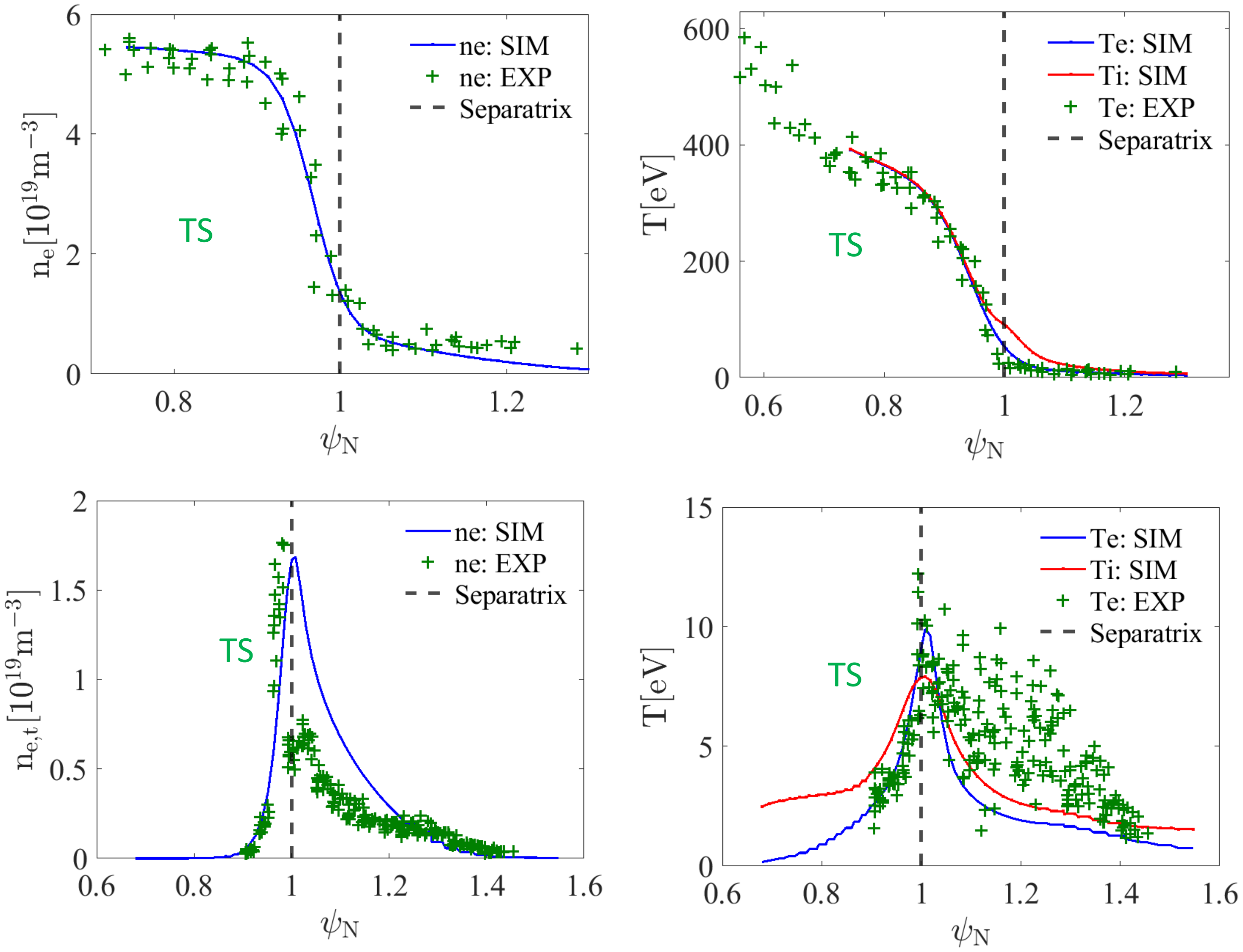

Detachment characteristics

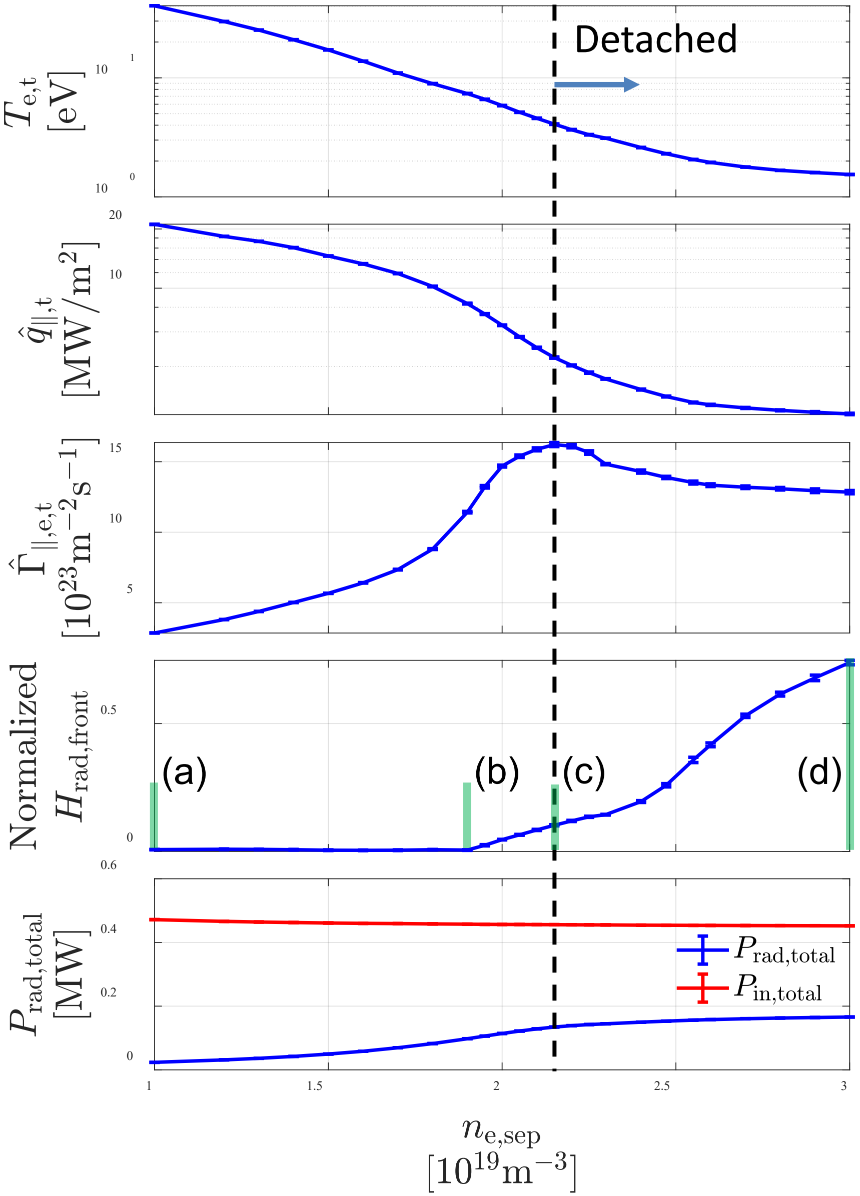

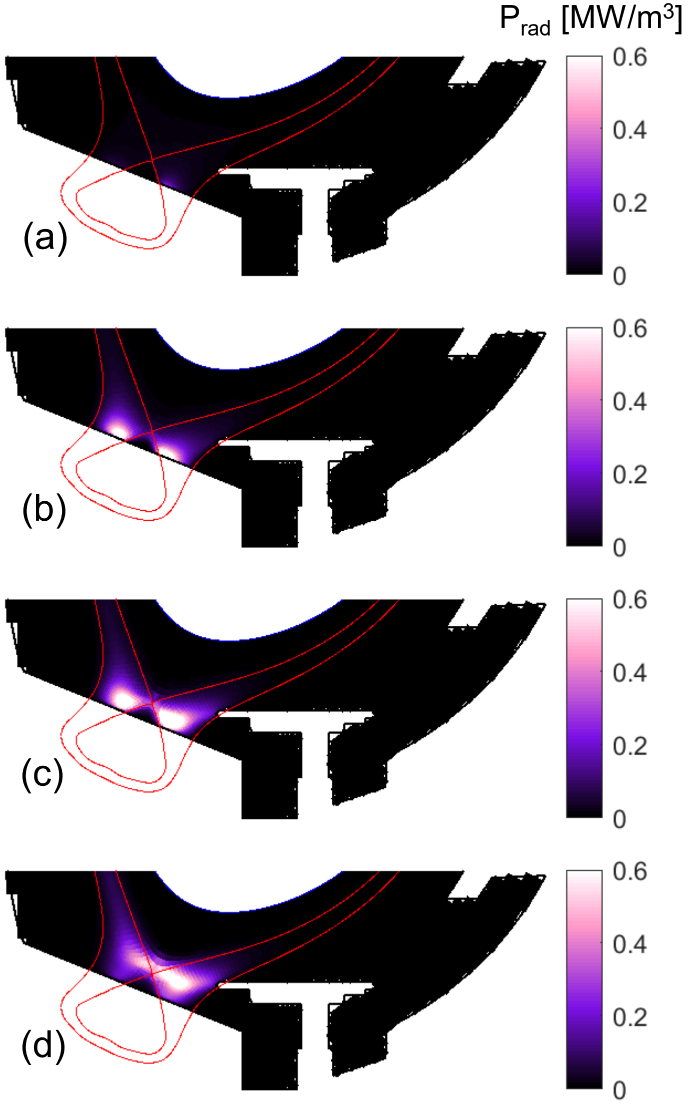

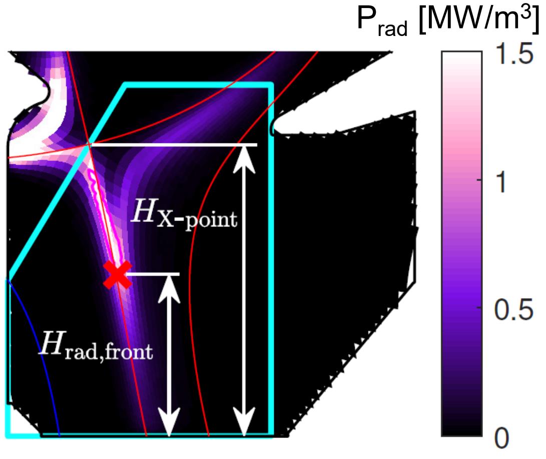

$$P_{rad,front} = 0.7P_{rad,max}$$

$$\text{Normalized } H_{rad,front} = H_{rad,front}/H_{X-point}$$

When detachment happens:

- Low target temperature (few eV), heat flux
- Rollover of particle flux (Constant P_{in}, low c_Z)
- Detach of radiation front
- High fraction of power radiated

Impact of baffle leakage in WEST

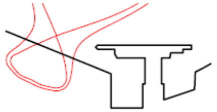
(a) Closed

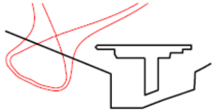
(b) Small

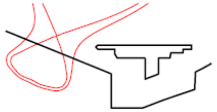
(c) Medium

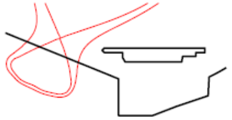
(d) Large


(e) open

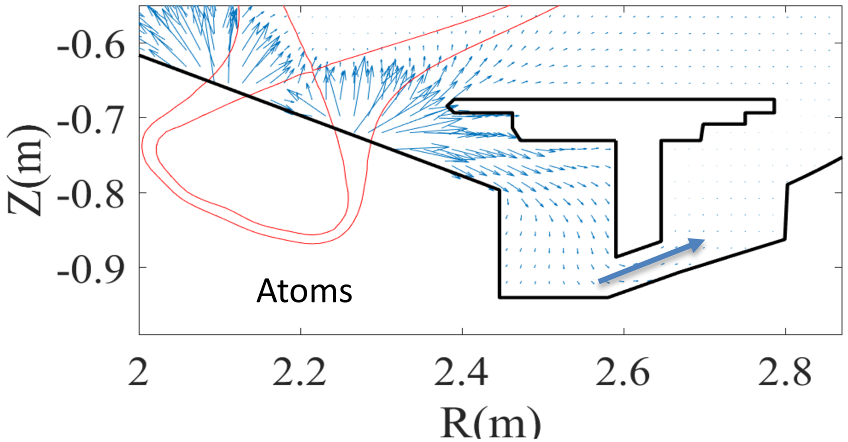

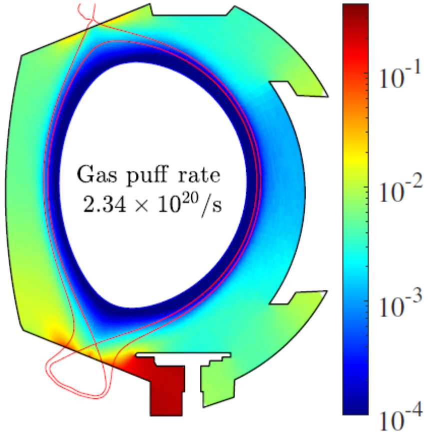

(a) $n_{\text{neu}}[1 \times 10^{19}\ /m^3]$

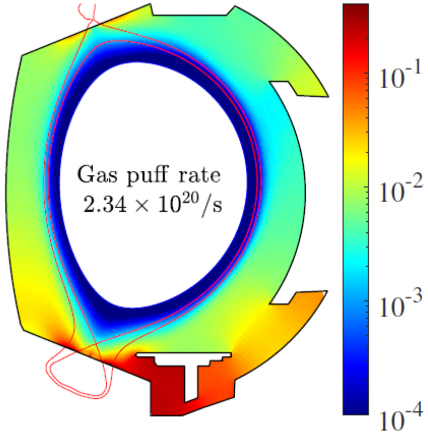

(b) $n_{\text{neu}}[1 \times 10^{19}\ /m^3]$

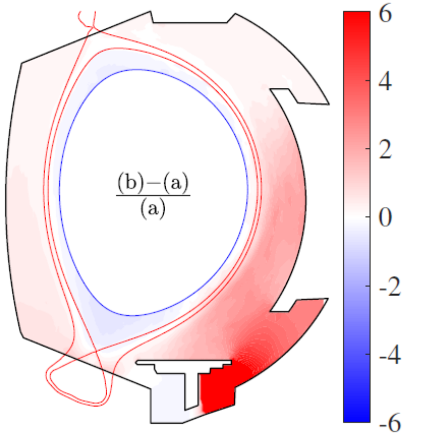

(c) Relative change rate

Impact of baffle leakage in WEST

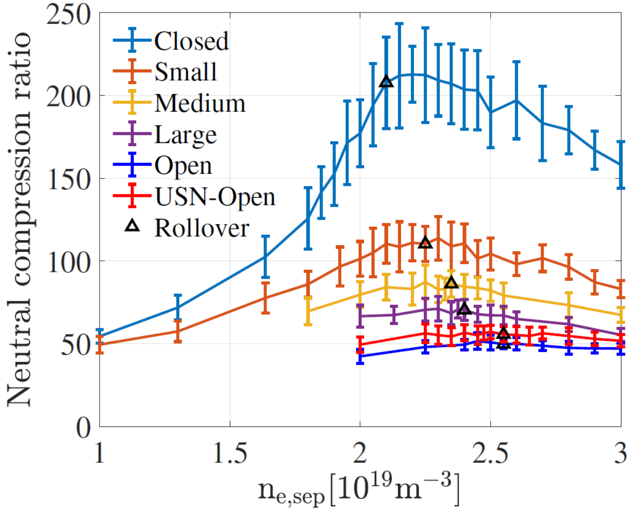

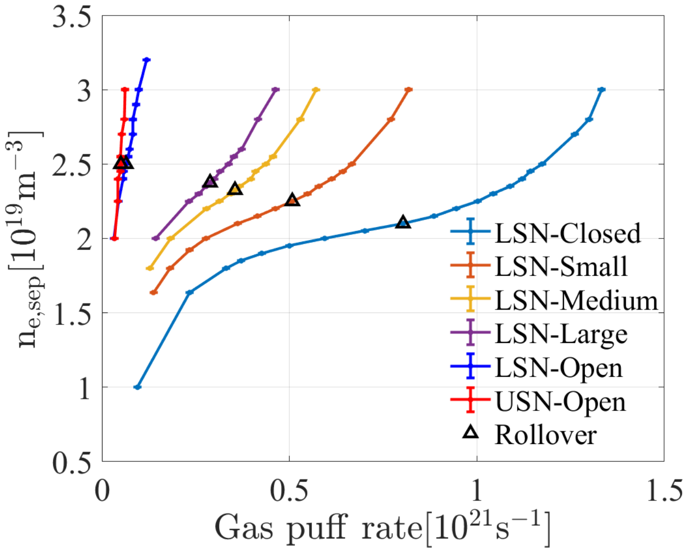

The case with less leakage:

- Better performance in trapping the neutral particles
- Higher neutral pressure near the target
- Greater momentum and power dissipation in the divertor
- Lower detachment threshold in $n_{e,sep}$

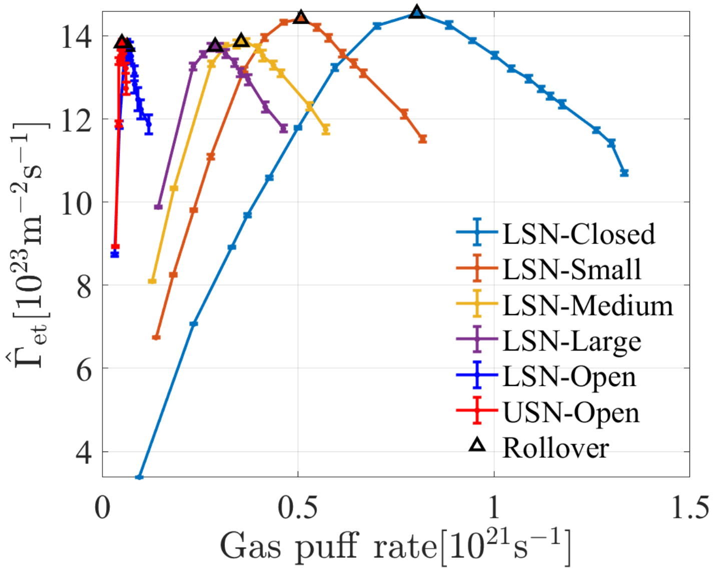

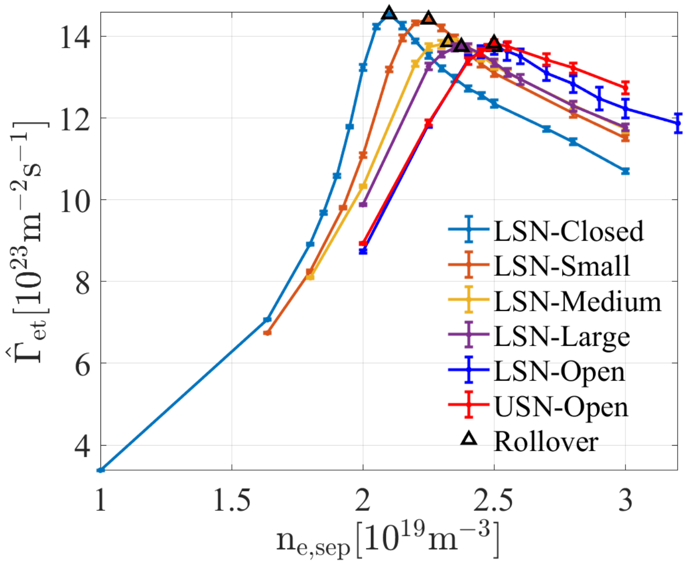

Impact of baffle leakage in WEST

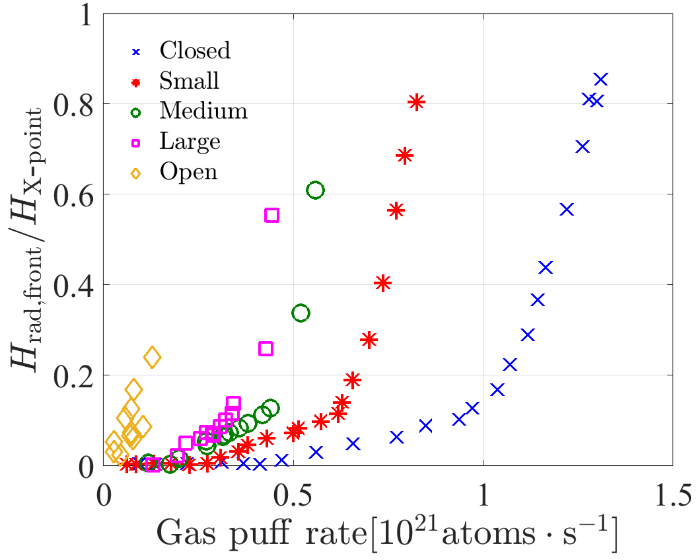

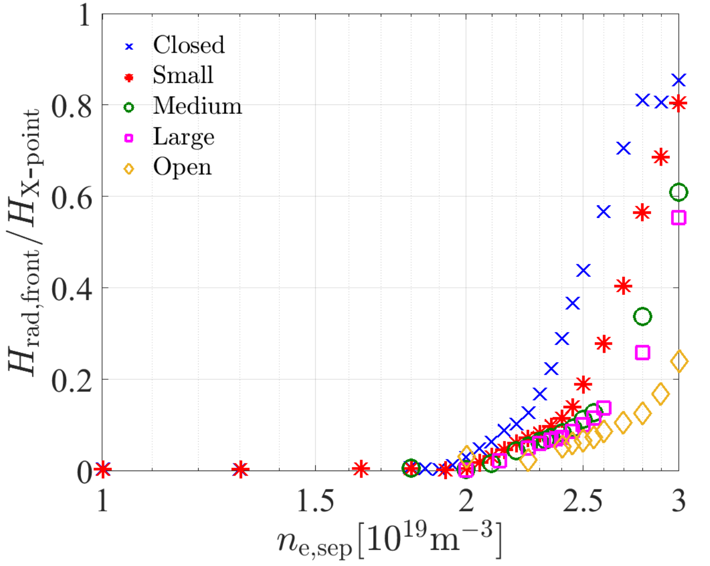

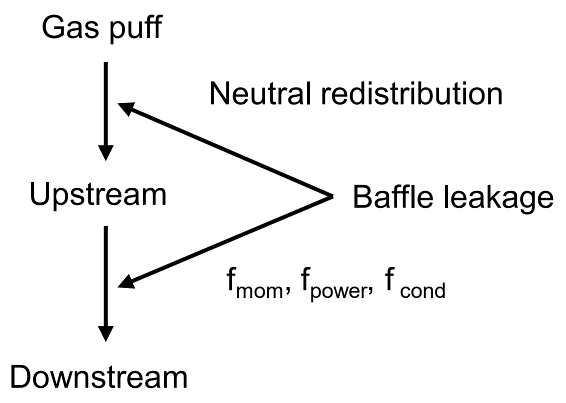

Gas puff

Neutral redistribution

Upstream

Baffle leakage

f_{mom}, f_{power}, f_{cond}

Downstream

Characteristic parameters of detachment:
$H_{rad,front}$, T_{et}, heat flux, particle flux (rollover)

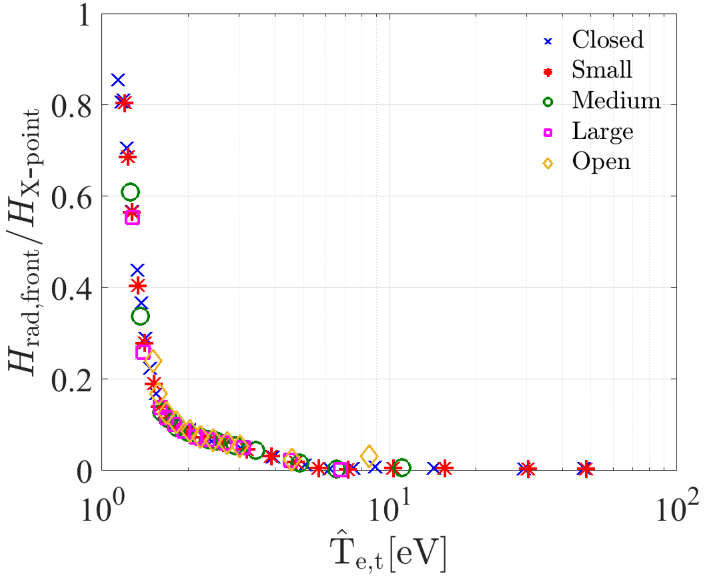

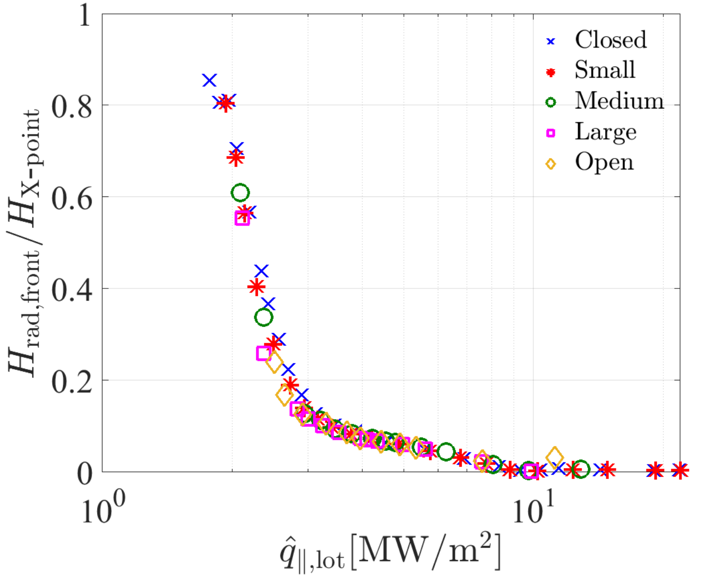

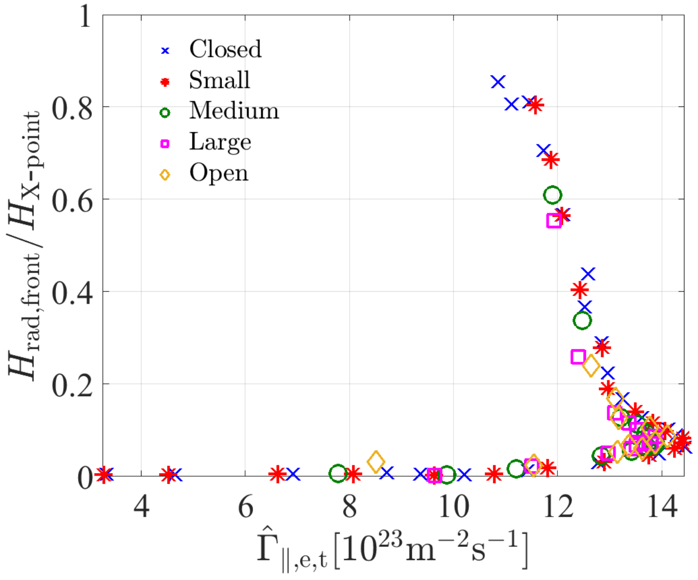

Impact of impurities: N seeding in TCV

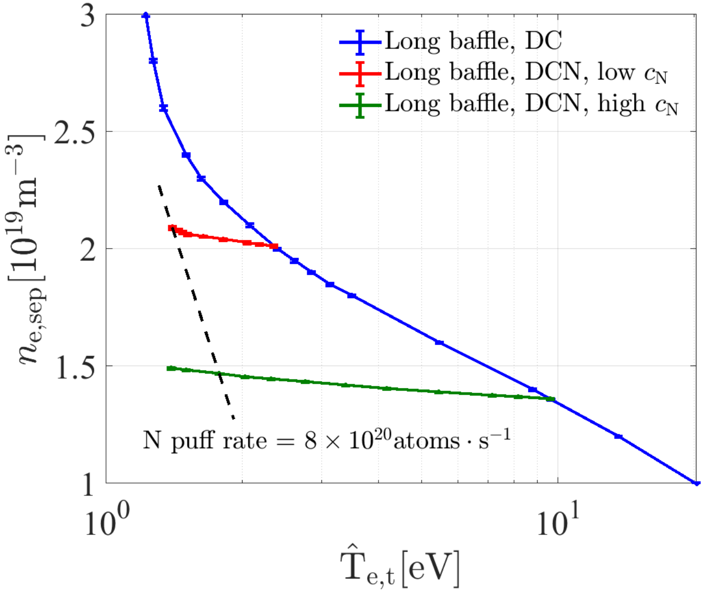

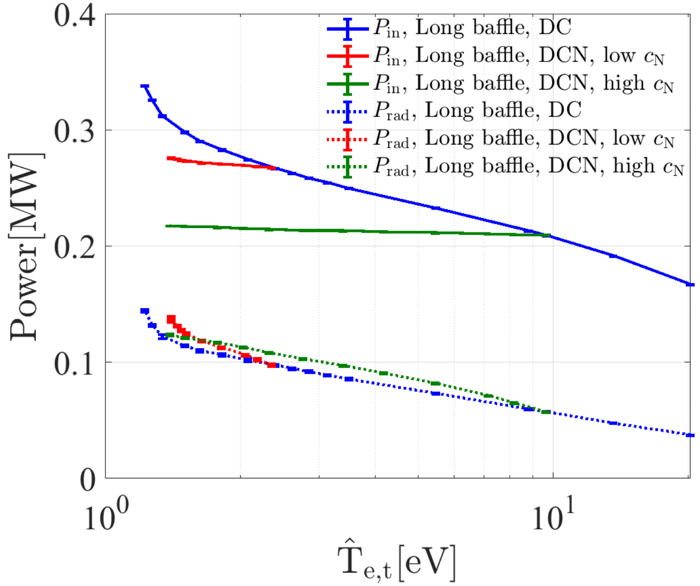

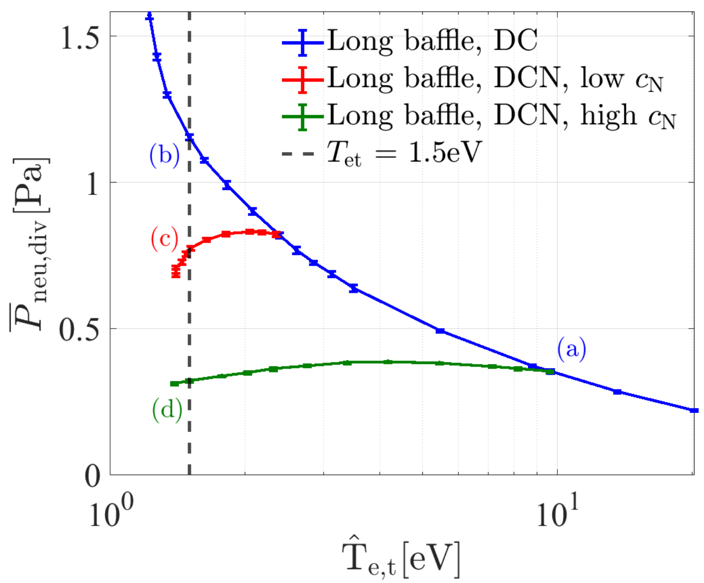

N seeding with the same core temperature:

- Maintain the same amount of power radiated with less input power required
- Reduce $n_{e,sep}$, $P_{neu,div,}$, when detached
- Radiate higher fraction of power

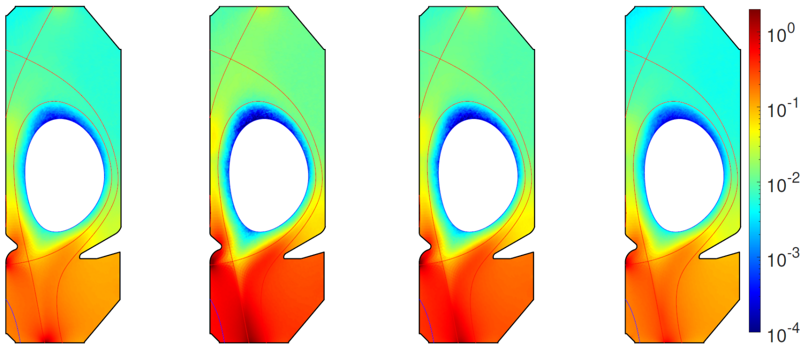

(a) DC, $\hat{T}_{e,t}$ = 9.6eV

(b) DC, $\hat{T}_{e,t}$ = 1.5eV

(c) DCN, low c_N, $\hat{T}_{e,t}$ = 1.5eV

(d) DCN, high c_N, $\hat{T}_{e,t}$ = 1.5eV

Pneu [Pa]

Impact of impurities: N seeding in TCV

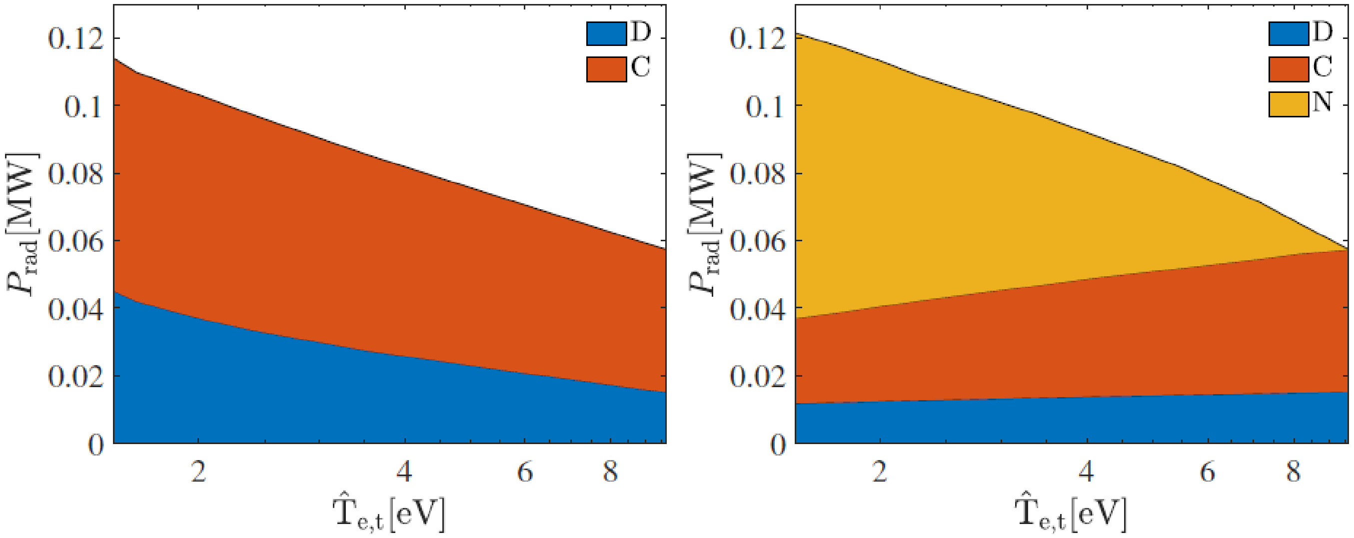

(a) D_2 puff scan (b) N puff scan, const. low D_2 puff

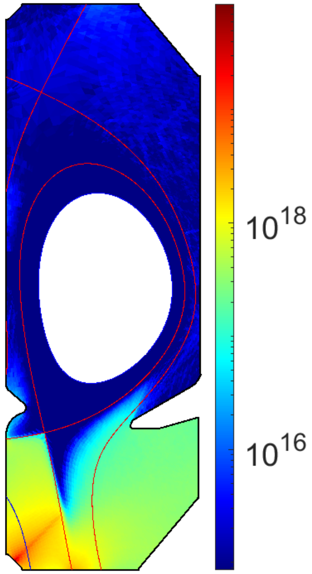

N density, all charge states

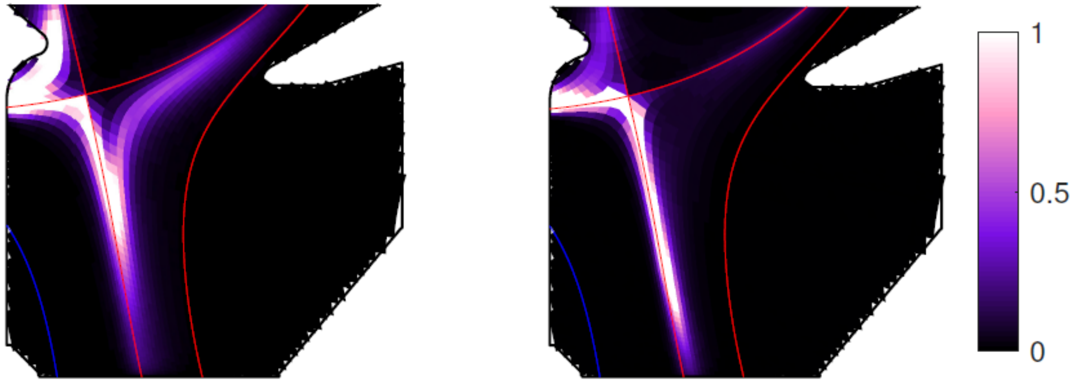

(a) Deep detached case without N puff (b) Deep detached case with high $C_{z,N}$

- Nitrogen accumulates in the region of low temperature close to the target
- Lower the height of the radiation front (high c_N case)

Impact of impurities and baffle closure in TCV

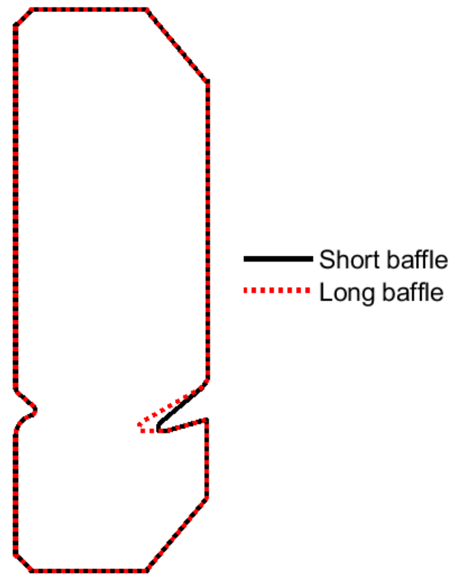

- Different baffle length cases detach at similar target temperature threshold
- Long baffle case with different c_Z detach at similar parallel heat flux threshold

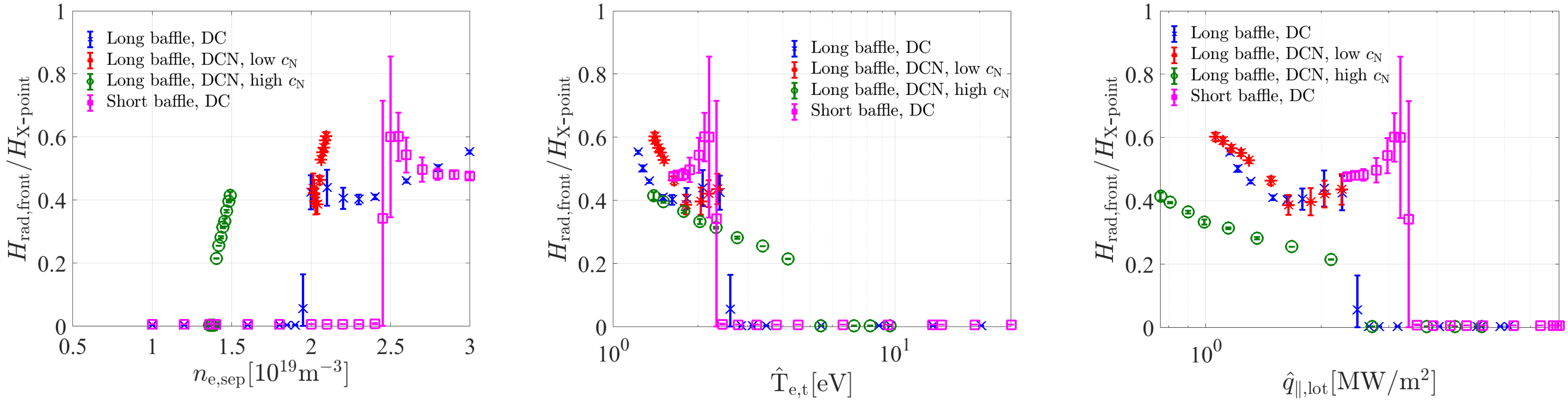

Simplified model: semi-detachment prediction

$$\mathrm{LHS} = \mathrm{P_{sep}/R_{det,point}}$$

$$\mathrm{RHS} = \frac{1}{1.3}\,\mathrm{p_0}(1+\mathrm{f_z c_z})\cdot\left(\lambda_{\mathrm{int}}/0.005\mathrm{m}\right)\cdot(\mathrm{R}/1.65\mathrm{m})^{\mathrm{r}}\times\left[\mathrm{MWm^{-1}\cdot Pa\cdot m}\right]$$

$$q_{det} = \mathrm{LHS/RHS}$$

- Based on an experimental formula (least-squares fitting of nonnegative functions of Tdiv versus Psep/R and the weighted pressures)
- Arbitrary-sized device with closed divertor
- high values of $\mathrm{f_z c_z}$ (saturation of the divertor radiation)
- Semi-detached when q_{det} =1, verified in AUG

[A Kallenbach et al 2016 PPCF 58 045013]

P_{sep}	Overall power through SEP
$R_{det,point}$	0.8 m (position of outer strike point)
P_0	Mean neutral pressure under baffle (marked by blue)
f_z	18 (Relative efficiency of N for detachment achievement compared to deuterium)
c_z	$P_{neu,N,div}/P_{neu,D,div}$ (Ratio of mean pressure along divertor outer leg)
λ_{int}	L_int = lambda_q+1,64S S~lambda_q/2 (lambda_q is evaluated on the OMP profile)
R	0.9 m (Major radius)
r_z	0,1 (weak exponent of N for the size dependence of detachment onset)

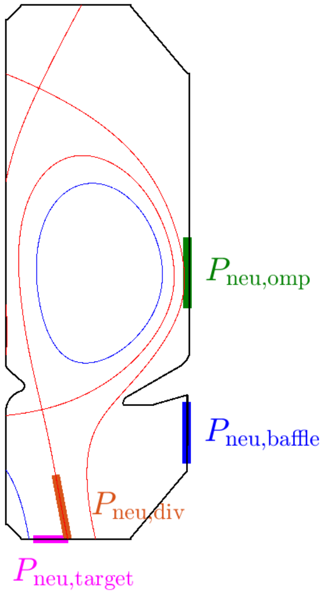

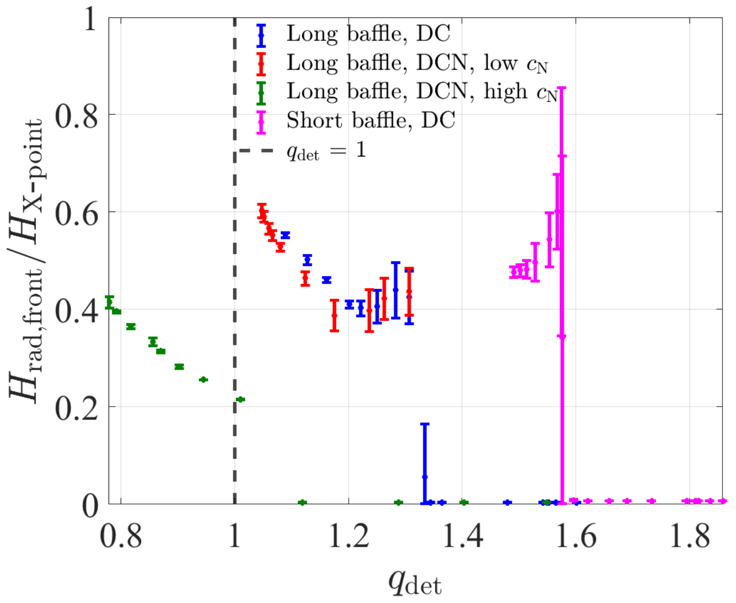

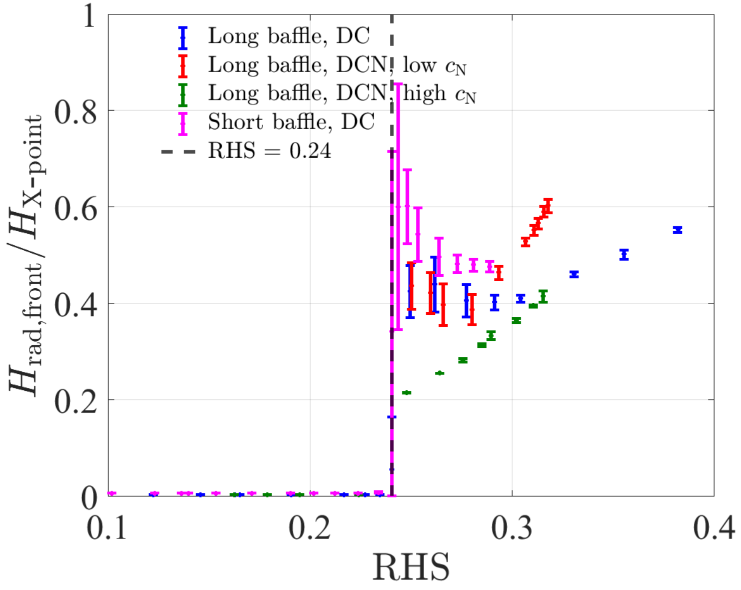

Simplified model: XPR prediction

$$X_A = \frac{P_{ion} + P_{CX}}{P_{cond}} \sim n_{0,X} n_{e,u} f_{exp} B_{t,u}^2 / (T_{e,u}^{2.5} B_{\theta,u}^2)$$

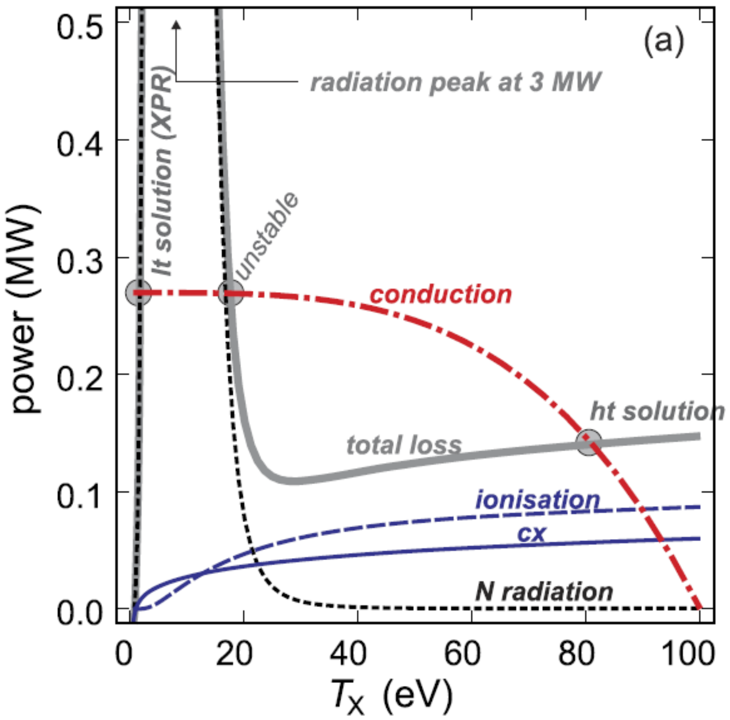

[U. Stroth et al 2022 NF 62 076008, Ou Pan et al 2022 NF]

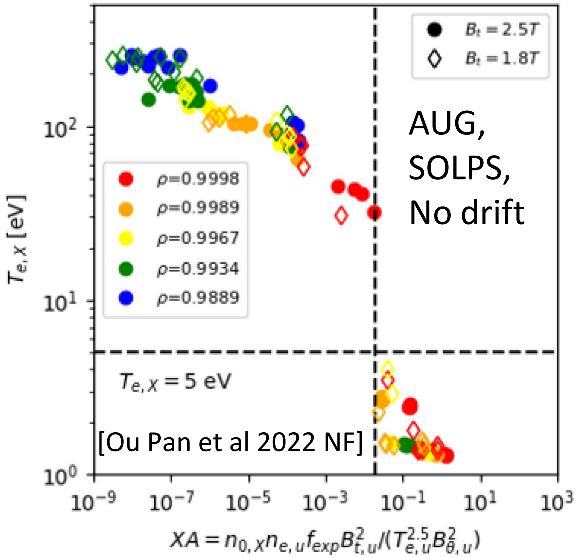

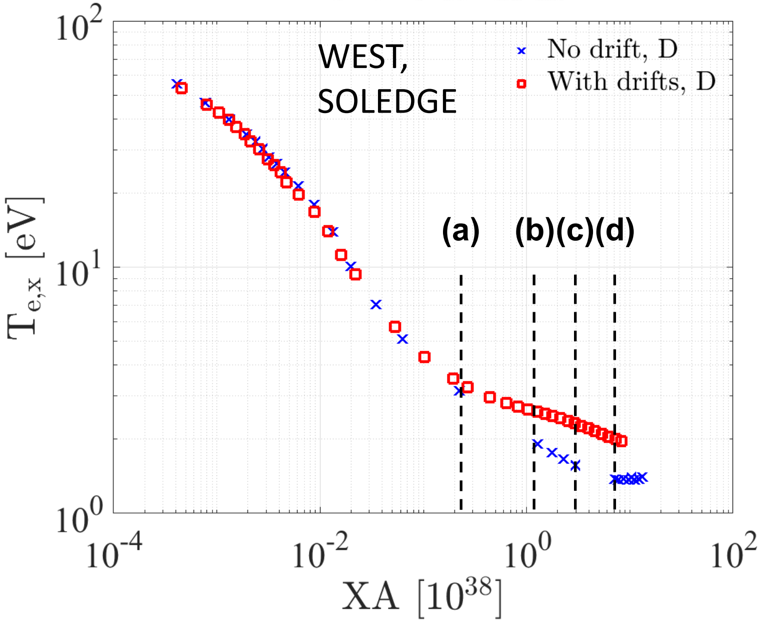

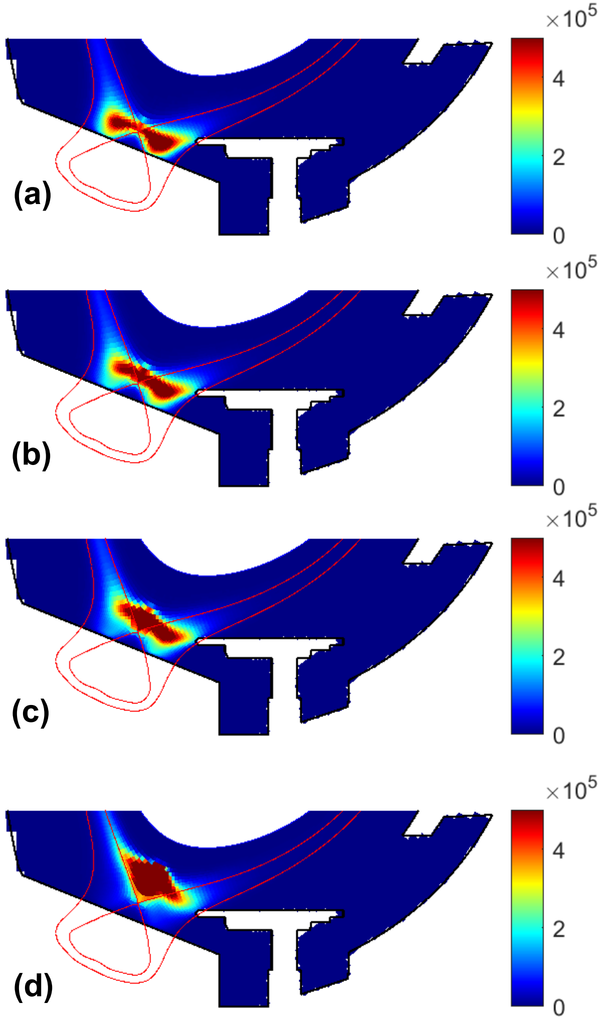

Detachment control: LP

Saturate current of LP

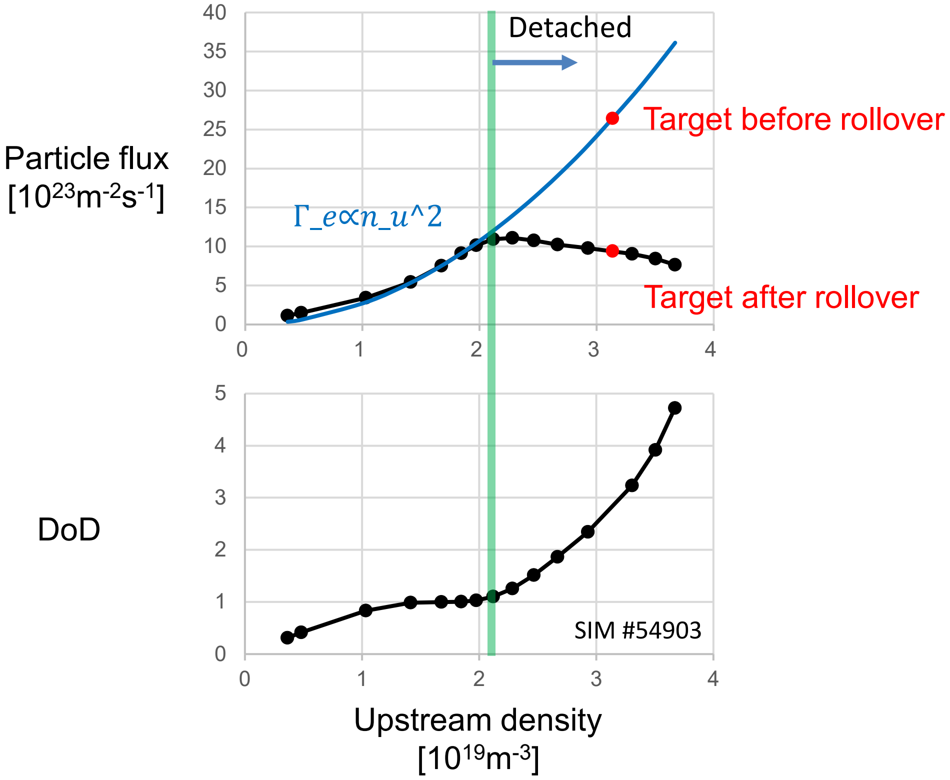

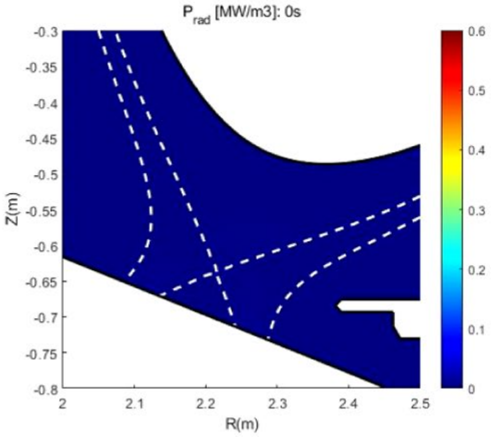

Detachment with particle flux controlled

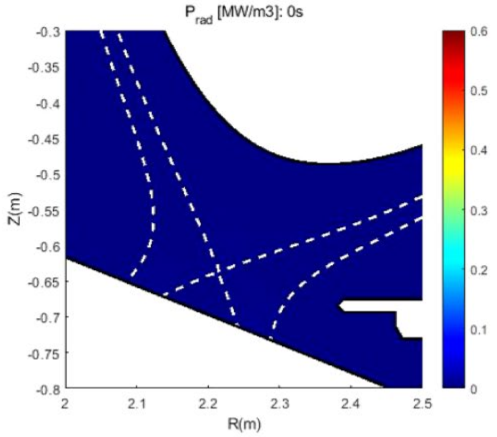

Detachment with upstream density controlled

Similar strategies were used in JET, EAST, DIII-D, KSTAR
[Eldon 2022 PPCF, C Guillemaut 2017 PPCF, etc.]

Detachment control: Bolometry

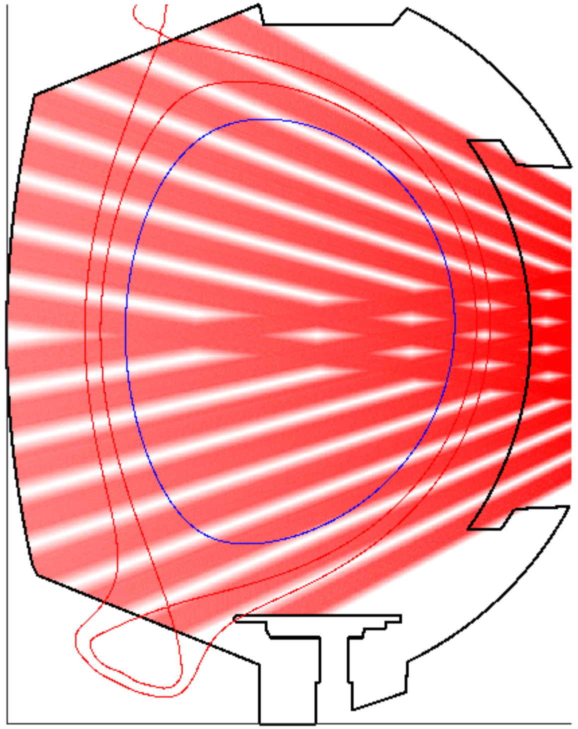

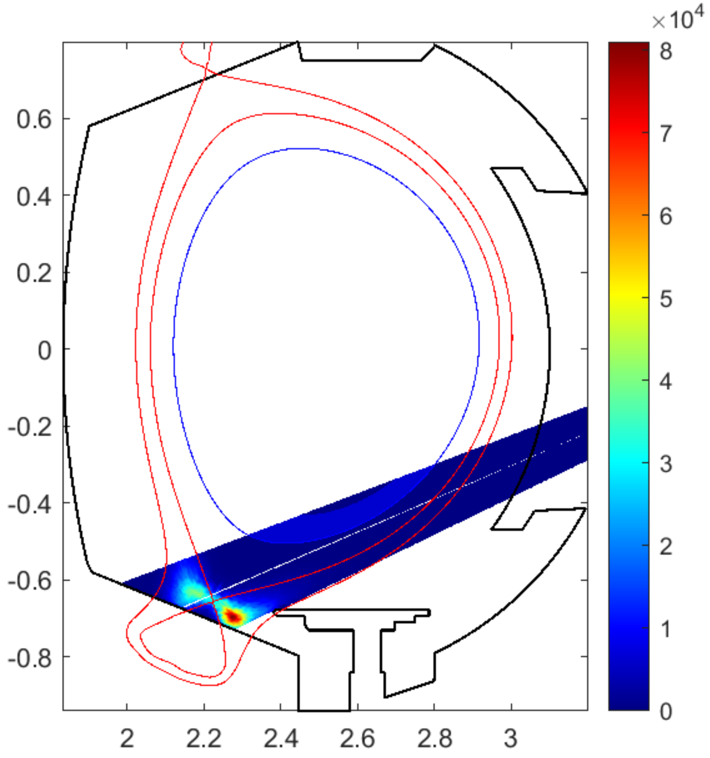

Posttreatment based on Syndi
[P Devynck 2021 J. Phys. Commun]

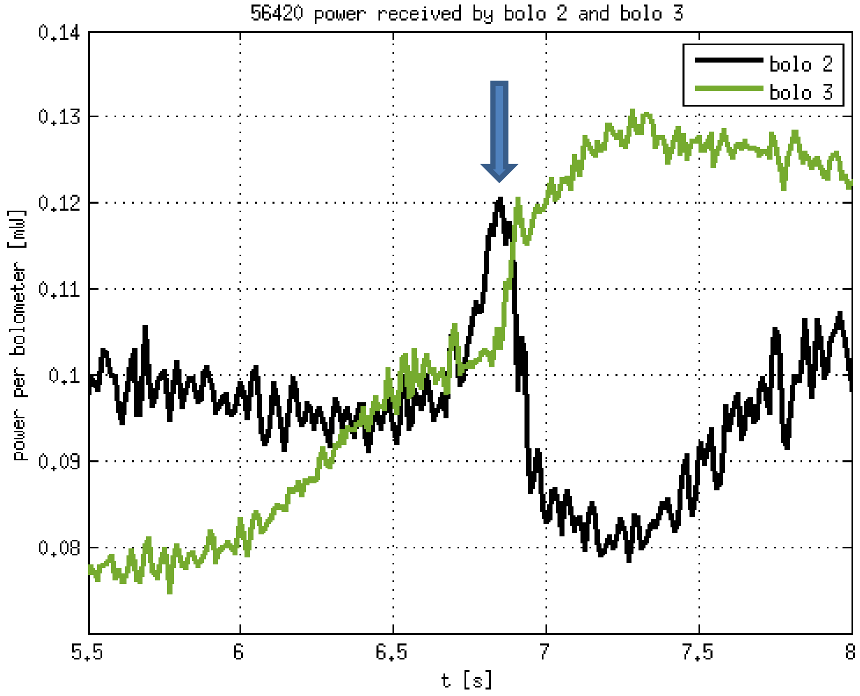

Detachment control: Time delay

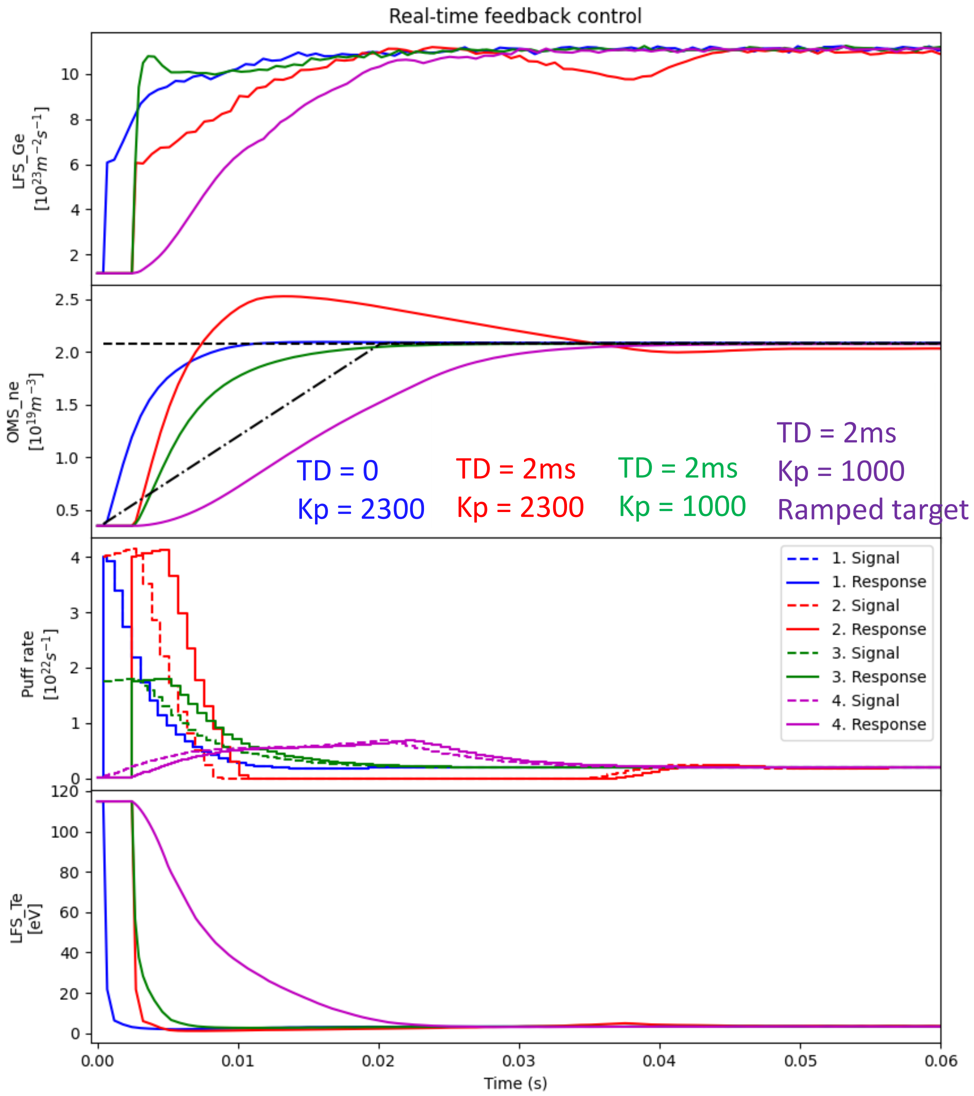

Suppose:
Puff frequency >= data sampling frequency

- The feedback control is still effective with high gain value when the time delay is less than 5ms
- Time delay influence can be mitigated by decreasing the gain value or using ramped target as a buffering

Detachment control

Items	Measurements	Controllable plasma		Detachment threshold			Comments
		Pure D or Low c_Z	High c_Z	Baffle leakage WEST	Baffle closure TCV	Impurities TCV	
Gas puff	🟩						Influenced by wall saturation state
Upstream SEP density	Reflectometry	🟩					Narrow range for cases with impurities
Target temperature	<5eV	🟩	🟩	2.4eV	2.4eV	Low c_Z	Detachment dependent para
Parallel heat flux	IR	🟩	🟩	4.2MW/m^2		2.7MW/m^2	Detachment dependent para
Normalized radiation front height	▨	🟩	🟩	0.1			
Target saturate current	LP	Fixed P_{in}		Rollover			No obvious rollover with high cZ
Divertor neutral pressure	Baratron gauges	🟩					
q_{det}	c_Z		🟩				ideal situation
RHS	c_Z	🟩	🟩		0.24	0.24	Consistent threshold for TCV cases
Prad,div	Bolometry	▨	▨				Short time delay
Line integral density near X point	Interferometry	🟩	▨				
XA	$P_{0,X}$	🟩	▨			1.14×10^{34}	

▨ Under investigation

Conclusion

- Radial non-constant transport coefficients obtained by the feedback control method are applied in the simulation, allowing a better match with experimental results
- The detachment process is reproduced through the SOLEDGE-EIRENE transport code
- The impact of multiple factors on detachment properties in WEST/TCV is investigated
- Some parameters are found to be highly related to detachment, and its threshold value is not influenced by baffle closure or impurities concentration
- Next step: High input power case, WEST case with impurities, and more diagnostic methods

The end

THANK YOU FOR YOUR ATTENTION

Detachment control

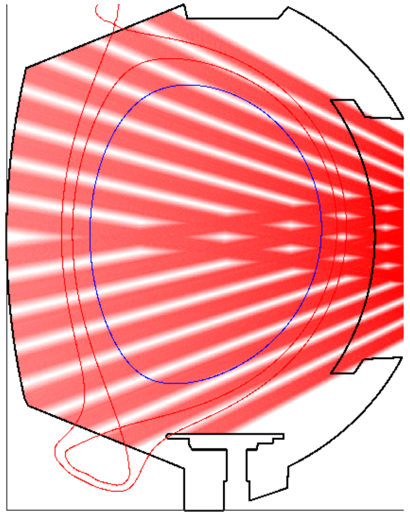

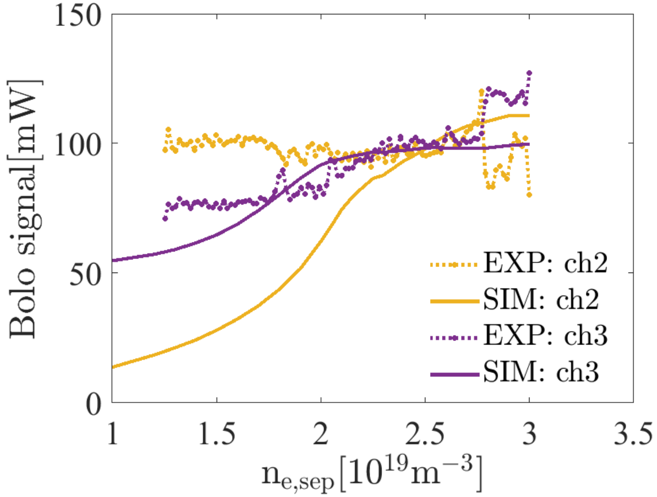

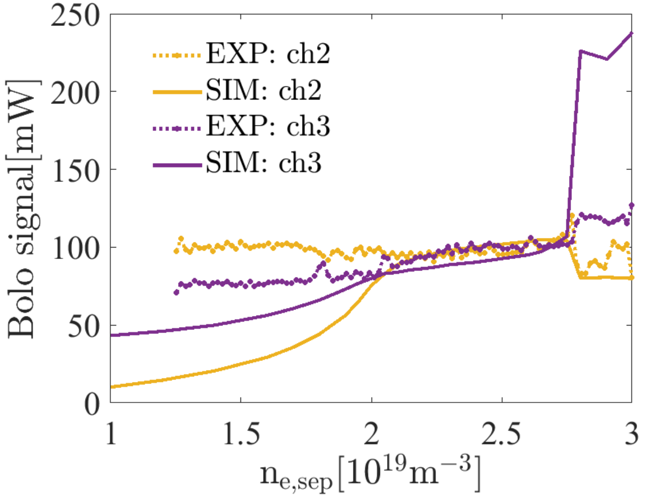

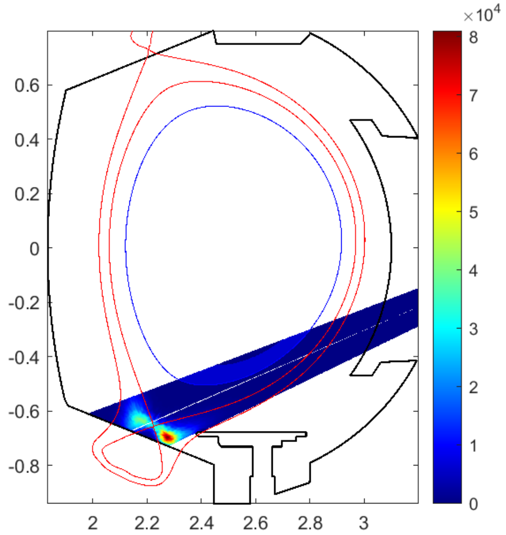

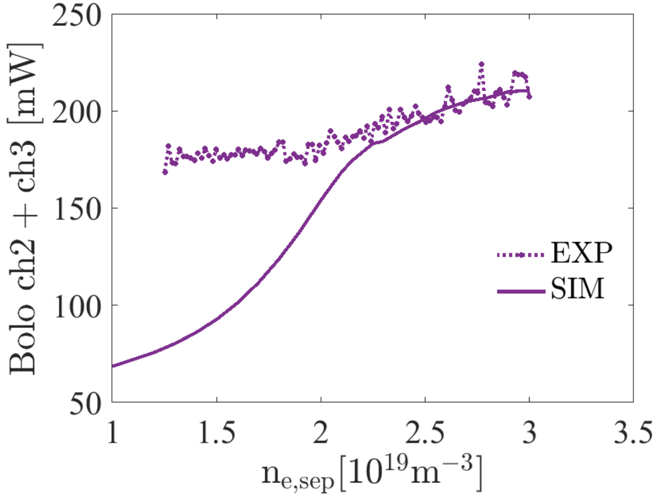

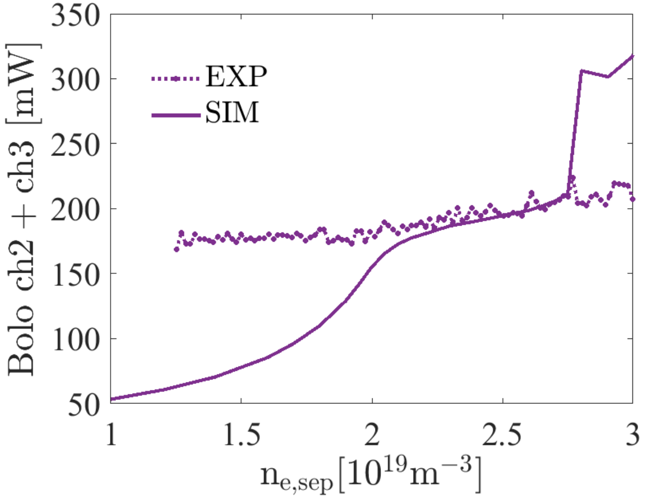

Annex: WEST

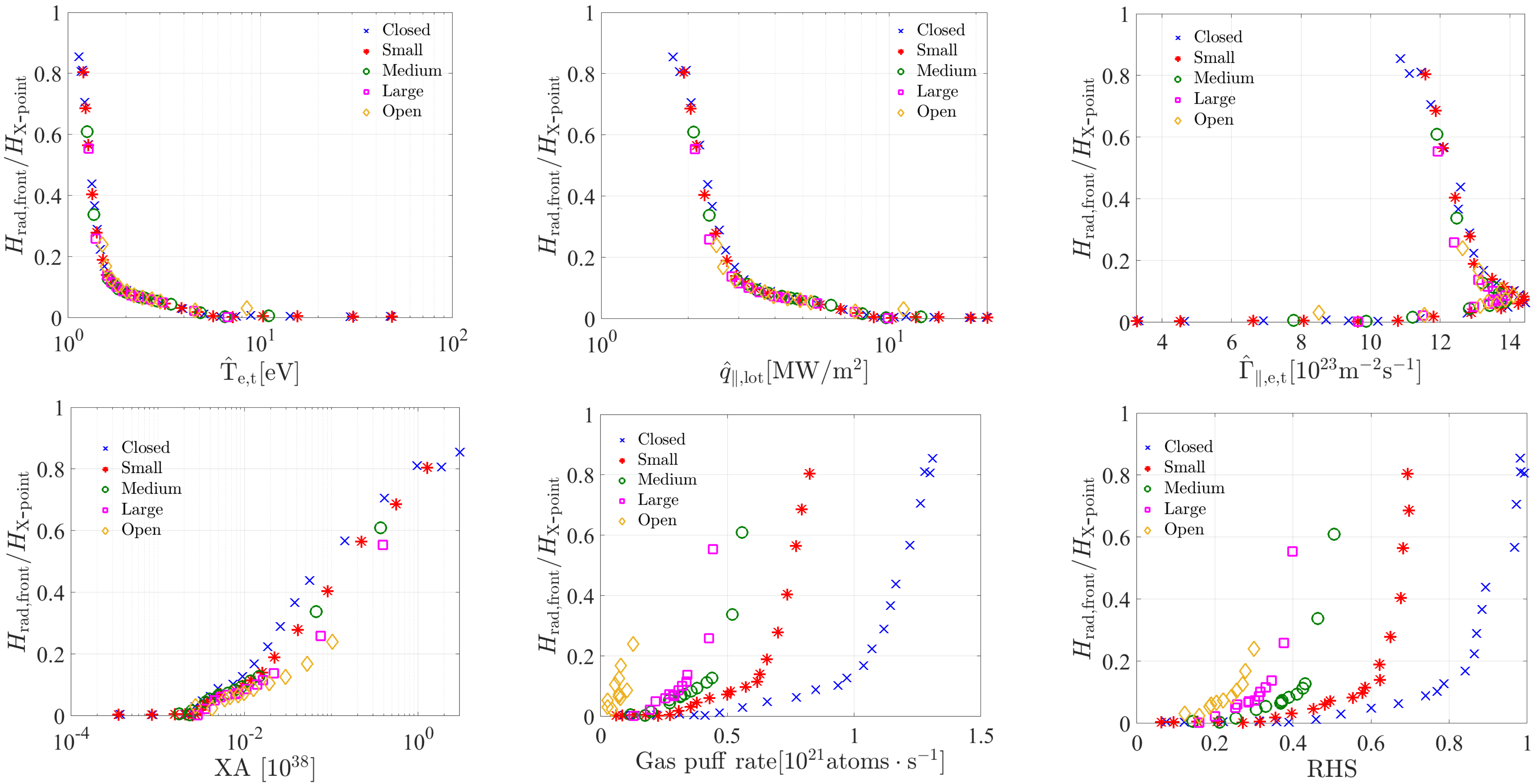
Closed
Small
Medium
Large
Open
$H_{\mathrm{rad,front}}/H_{\mathrm{X\text{-}point}}$
$\hat{T}_{e,t}\,[\mathrm{eV}]$
$\hat{q}_{\parallel,\mathrm{lot}}\,[\mathrm{MW/m^2}]$
$\hat{\Gamma}_{\parallel,e,t}\,[10^{23}\mathrm{m^{-2}s^{-1}}]$
XA $[10^{38}]$
Gas puff rate$[10^{21}\mathrm{atoms}\cdot\mathrm{s}^{-1}]$
RHS
0
0.2
0.4
0.6
0.8
1
10^0
10^1
10^2
10^{-4}
10^{-2}
4
6
8
10
12
14
0.5
1.5

Annex: TCV

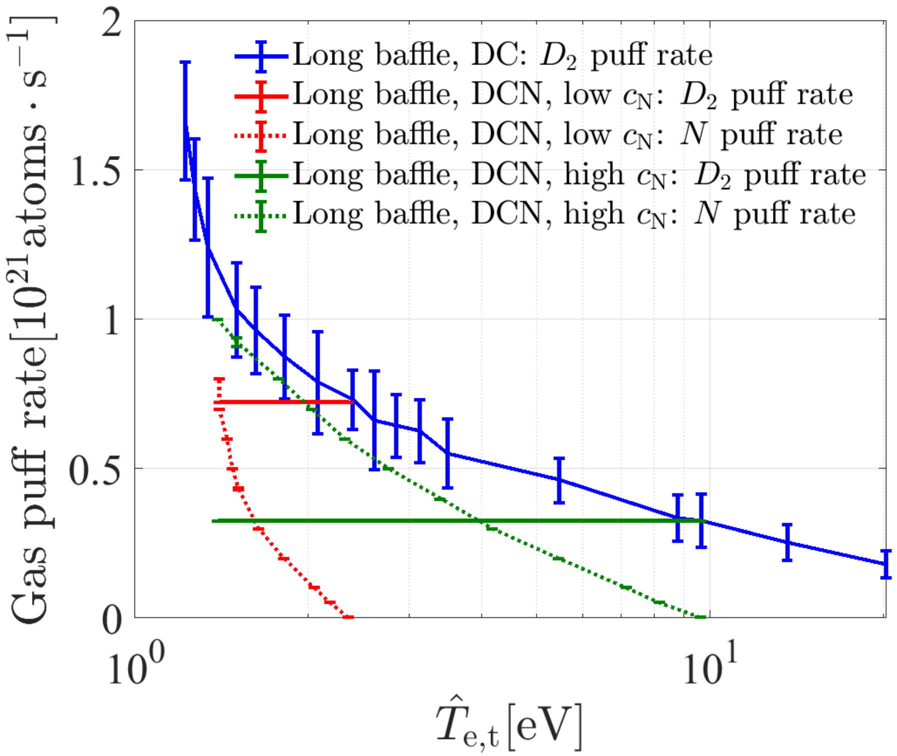
Long baffle, DC: D_2 puff rate
Long baffle, DCN, low c_N: D_2 puff rate
Long baffle, DCN, low c_N: N puff rate
Long baffle, DCN, high c_N: D_2 puff rate
Long baffle, DCN, high c_N: N puff rate
Gas puff rate$[10^{21}\text{atoms}\cdot s^{-1}]$
0
0.5
1
1.5
2
10^0
10^1
$\hat{T}_{e,t}$[eV]

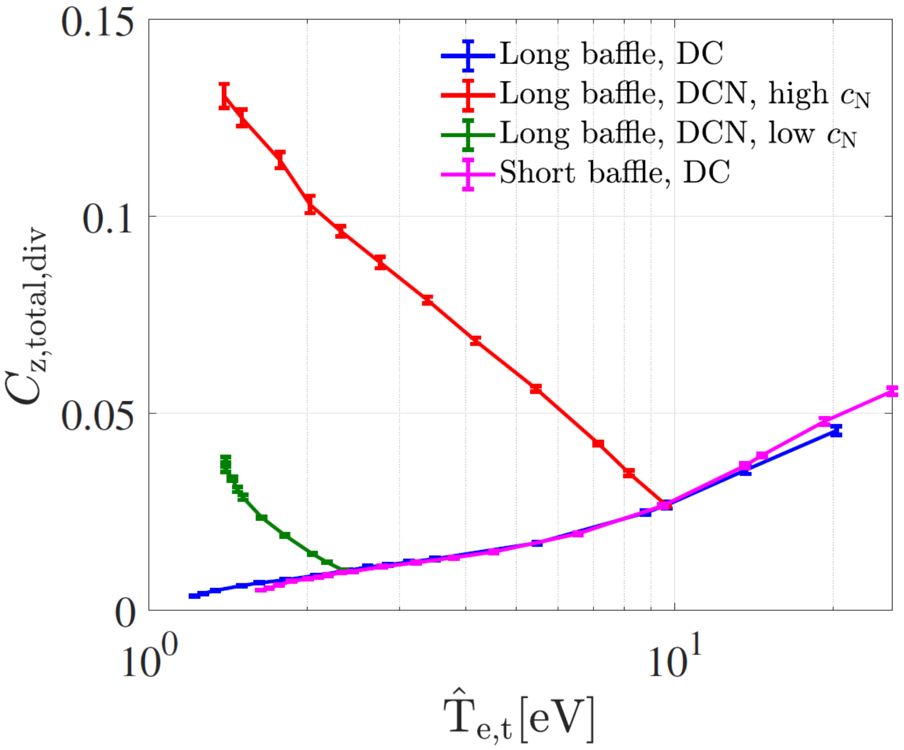
Long baffle, DC
Long baffle, DCN, high c_N
Long baffle, DCN, low c_N
Short baffle, DC
$C_{z,\text{total,div}}$
0
0.05
0.1
0.15
10^0
10^1
$\hat{T}_{e,t}$[eV]

Annex: TCV

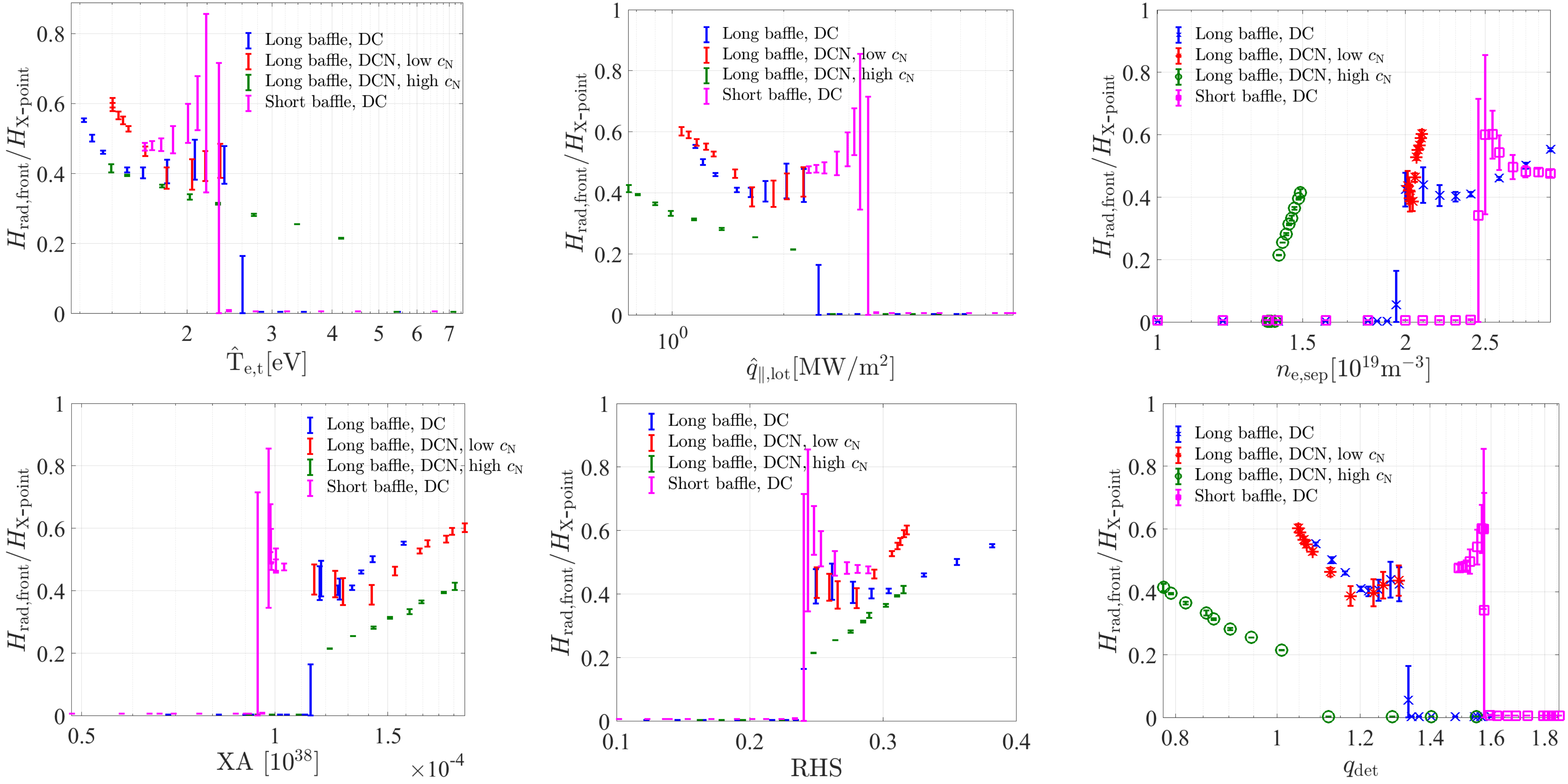

$H_{\mathrm{rad,front}}/H_{\mathrm{X\text{-}point}}$
Long baffle, DC
Long baffle, DCN, low c_N
Long baffle, DCN, high c_N
Short baffle, DC
$\hat{\mathrm{T}}_{\mathrm{e,t}}\,[\mathrm{eV}]$
0
0.2
0.4
0.6
0.8
2
3
4
5
6
7
$\hat{q}_{\parallel,\mathrm{lot}}\,[\mathrm{MW/m^2}]$
10^0
1
$n_{\mathrm{e,sep}}\,[10^{19}\mathrm{m^{-3}}]$
1.5
2.5
XA $[10^{38}]$
0.5
1.5
$\times 10^{-4}$
RHS
0.1
0.2
0.3
0.4
q_{det}
1.2
1.4
1.6
1.8

Numerical modeling: WEST L-mode, real-time scan compare

Gas puff rate

Upstream density

Line integral density near X-point

Peak ion flux at OT

Peak T_e at OT

Peak n_e at OT

Peak parallel heat flux at OT

Neutral pressure under baffle

Input power and Radiated power

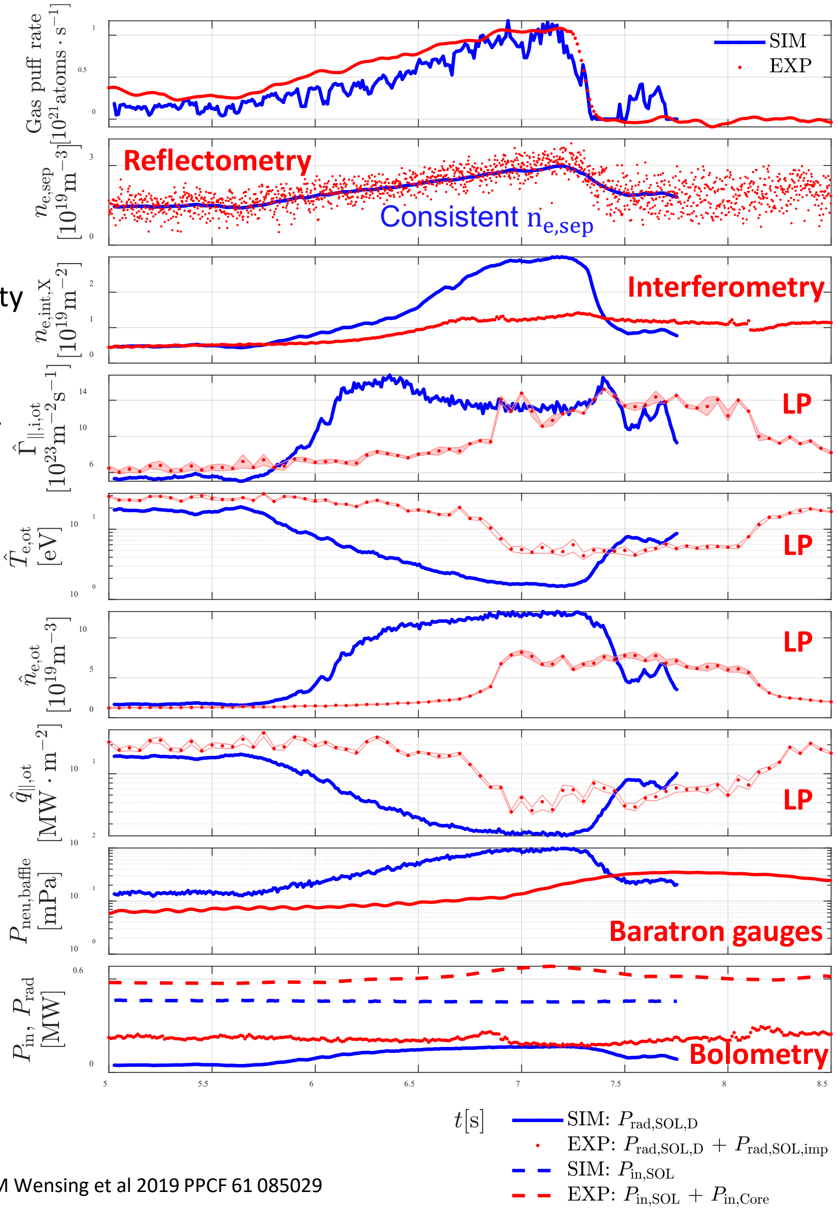

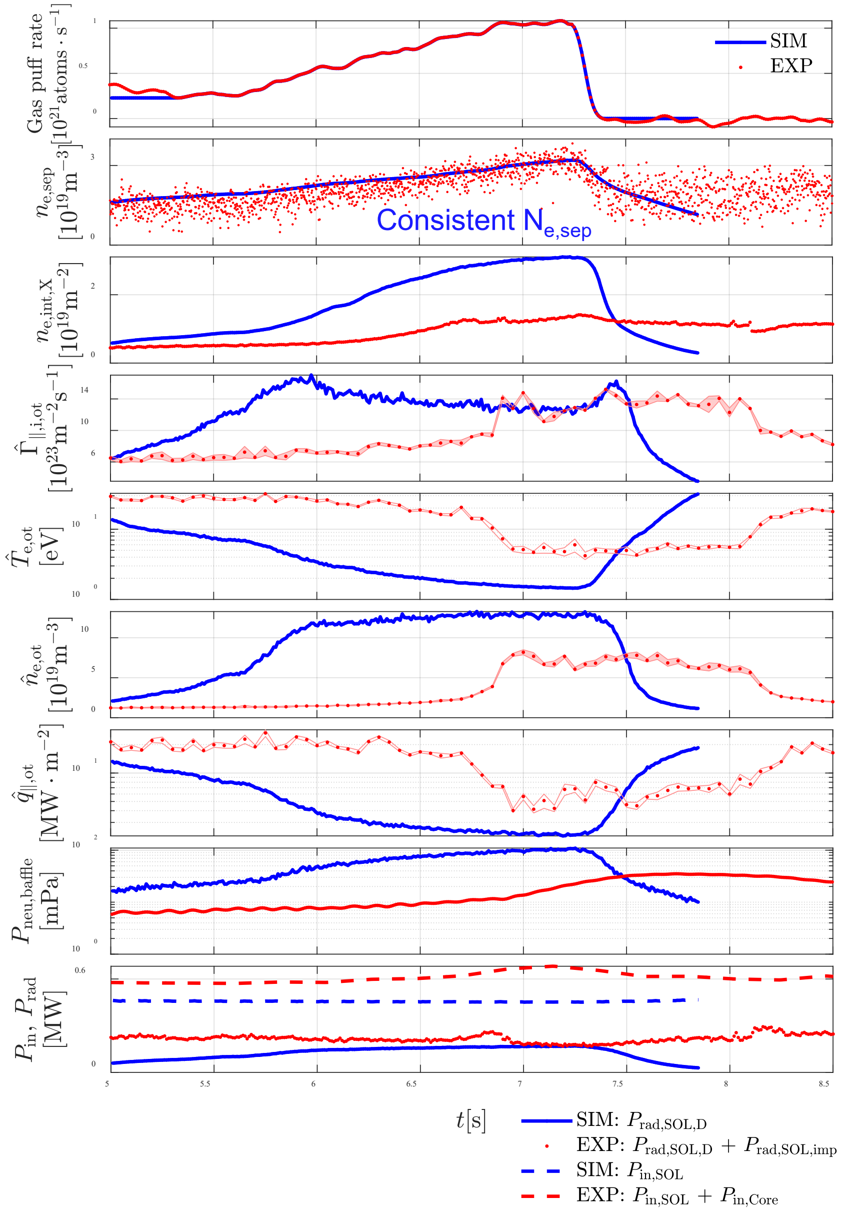

P_{neu} recalculated based on M Wensing et al 2019 PPCF 61 085029

Impact of drifts

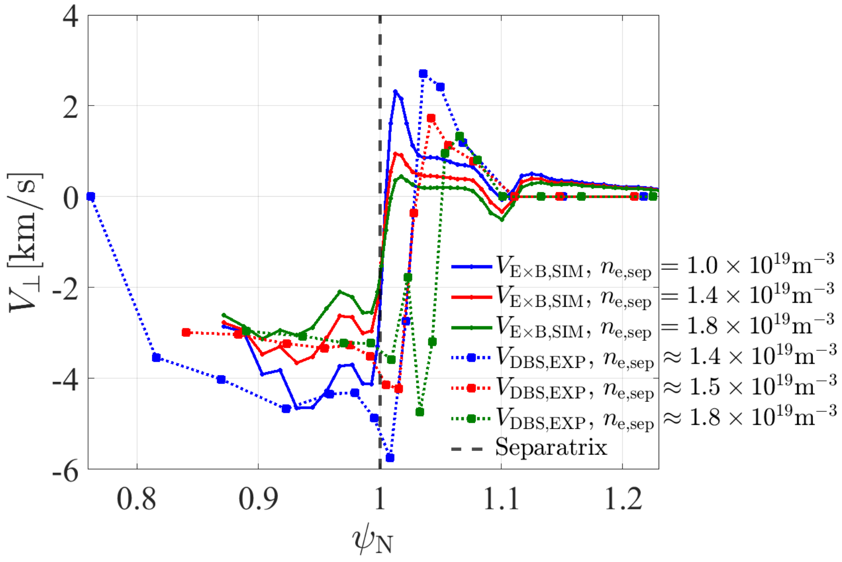

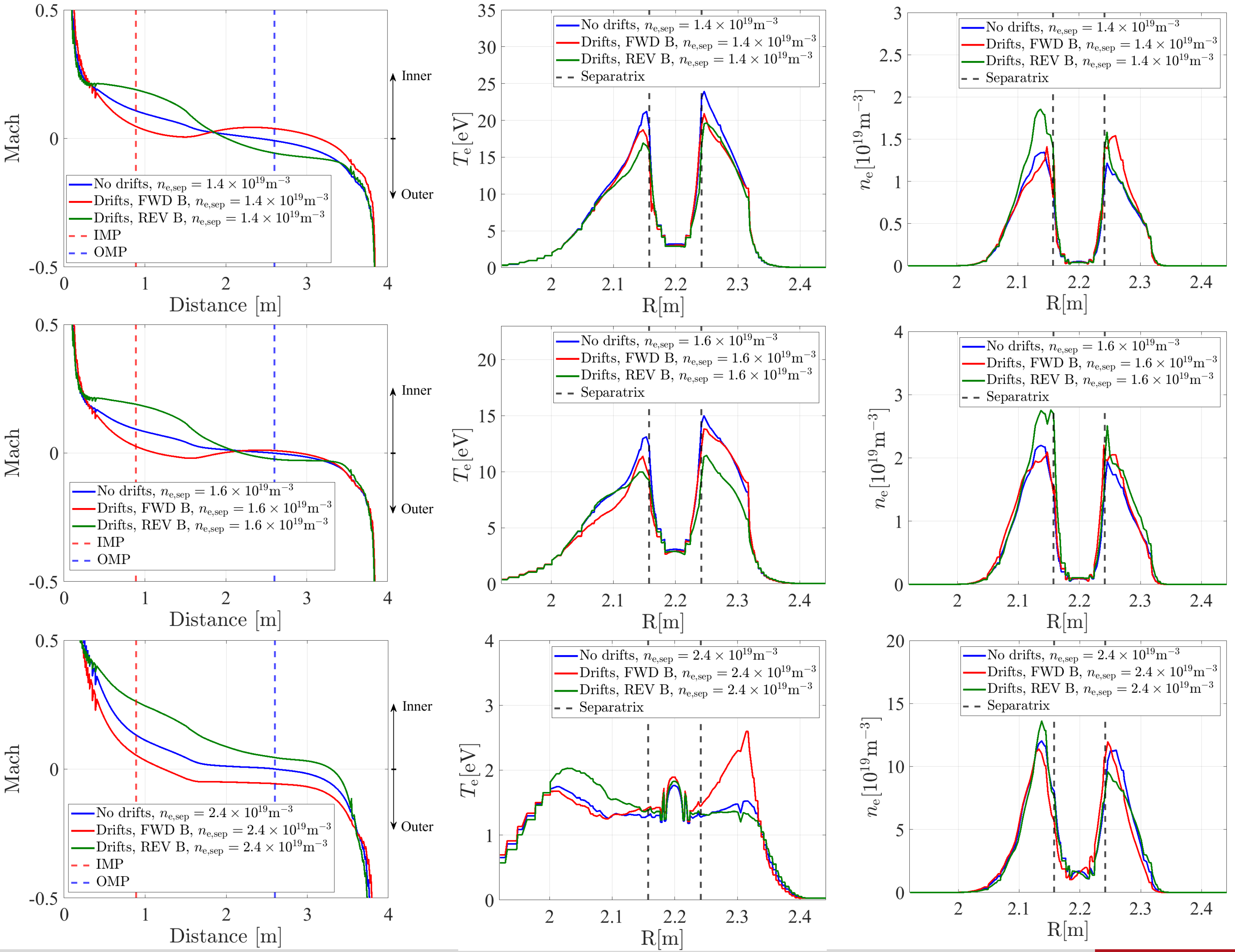

- Mainly influence the LFS
- The stagnant point of LFS moving toward the inner target
- More power flow into the outer target, increasing the Te
- Higher the detachment threshold
- The peak of density profile closer to SEP on outer target

Impact of impurities: Oxygen in WEST

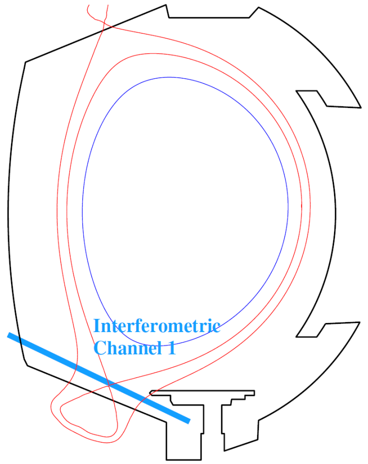

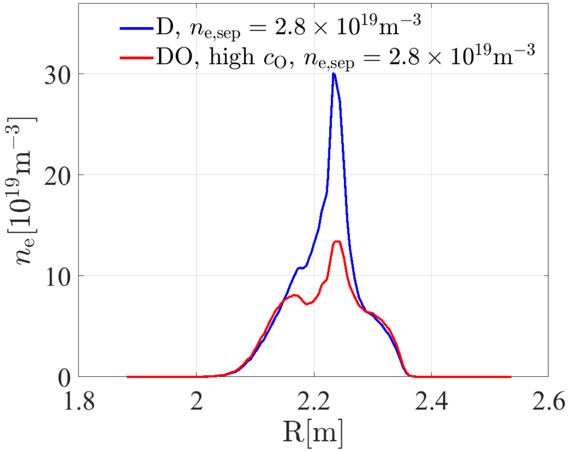

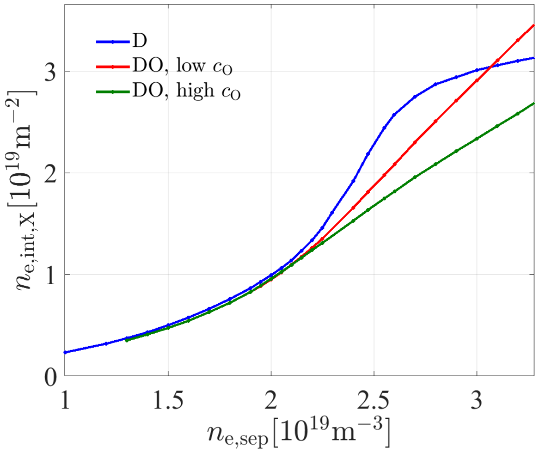

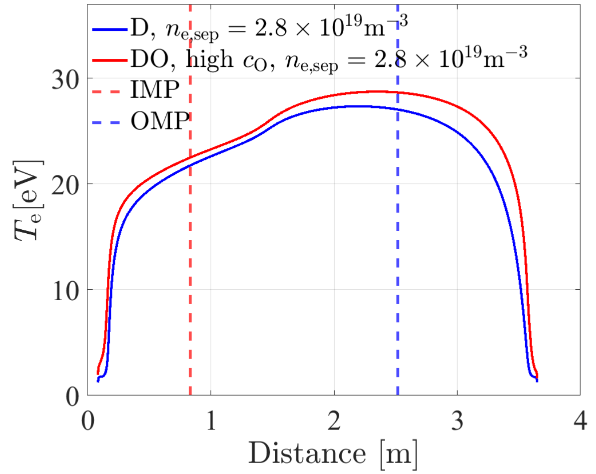

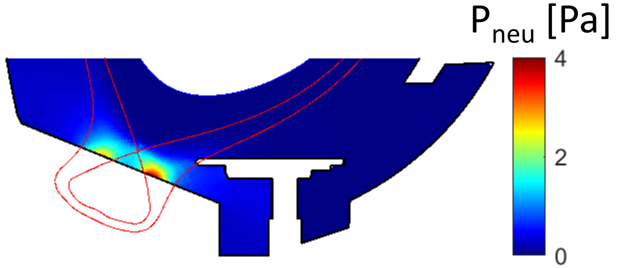

D, $T_{e,t}$ = 1.7eV

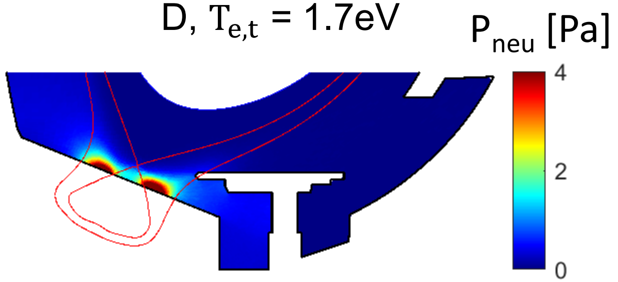

DO, high c_O, $T_{e,t}$ = 1.7eV

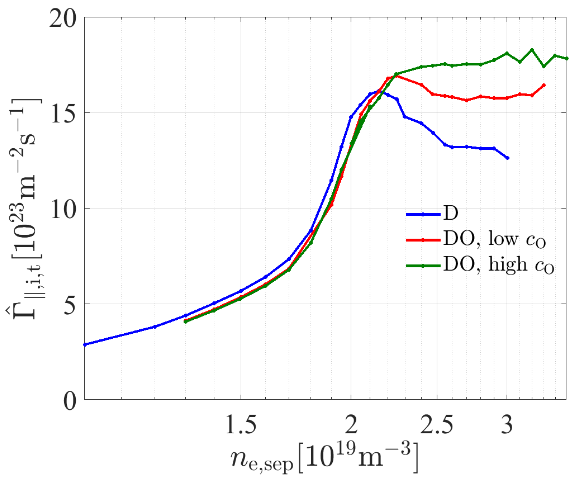

Oxygen seeding from the core
With constant input power (0.25%, 0.75%)

- Increase the temperature along SEP
- Lower the plasma density, and neutral pressure near X-point
- Delay or prevent the rollover of particle flux at the outer target